5-2020

Microbiome Diversity and Differential Abundances Associated with BMI, Immune Markers, and Fecal Short Chain Fatty Acids Before and After Synbiotic Supplementation

John Sterrett
East Tennessee State University

W Andrew Clark
East Tennessee State University

Michelle Chandley
East Tennessee State University

Microbiome Diversity and Differential Abundances Associated with BMI, Immune Markers, and Fecal Short Chain Fatty Acids Before and After Synbiotic Supplementation

John Sterrett

April 22, 2020

An undergraduate thesis
submitted in partial fulfillment
of the requirements for the
Honors College
University Honors Scholars Program
and the
Department of Rehabilitative Sciences
Honors-in-Discipline Program at
East Tennessee State University

John Sterrett, Author	Date
Dr. W Andrew Clark, Faculty Mentor	Date
Dr. Michelle Chandley, Faculty Reader	Date

Contents

Abstract

The gut microbiota and its metabolites – namely short chain fatty acids (SCFAs) – interact with the digestive, immune, and nervous systems. Microbiota with disrupted composition are highly associated with obesity, gastrointestinal symptoms, and chronic inflammation. Levels of SCFAs in the feces can represent dynamics of the microbiota and represent one mechanism by which the microbiota interacts with its host. This study aimed to further our understanding of associations between microbiota bacterial diversity and SCFAs, immune markers, BMI, and GI symptoms and to identify bacteria that are differentially abundant in different BMI groups and with synbiotic supplementation. Data (SCFAs, immunoglobulins, body mass index, fecal fiber, fecal protein, measures of GI symptoms, and 16s RNA sequences, n=11) was extracted from a randomized control trial investigating the effects of synbiotic supplementation in non-celiac gluten-sensitive participants. QIIME2 was used to process 16s RNA data, analyze quantitative, qualitative, phylogenetic quantitative, and phylogenetic qualitative measures of alpha and beta diversity and to perform an analysis of composition of microbiomes (ANCOM) for identification of differential abundances. Multiple metrics of alpha diversity were found to significantly correlate with IgG4, IgM, IL-2, acetate, propionate, isobutyrate, valerate, isovalerate, caproate, heartburn, urgent need to defecate, and feelings of incomplete evacuation. Multiple metrics of beta diversity were significantly different between normal and overweight, normal and obese, and overweight and obese BMI classification groups. Beta diversity was also found to significantly correlate with IgG1, IgG3, IgG4, IgA, IL-6, IL-8, fecal fiber propionate, butyrate, heartburn, acid regurgitation, nausea and vomiting, bloating, abdominal distension, increased gas, and eructation. The synbiotic intervention did not significantly alter alpha or beta diversity. An ANCOM identified bacterial taxa differentially abundant with BMI shifts and synbiotic supplementation, though these taxa were not those included in the synbiotic. Findings demonstrate alpha and beta diversity associations with various SCFAs, GI symptoms, immune markers, and BMI, and the results of the placebo-controlled intervention suggest careful consideration of placebo contents moving forward. This research supports plans to apply analysis to larger sample sizes to elucidate changes microbial profiles that are associated with clinically relevant biomarkers and symptoms.

1 Background

1.1 Microbial Communities

Most locations on earth harbor communities of microbes referred to as microbiomes [1]. The organisms that make up microbiomes are referred to as the "microbiota", though the terms "microbiome" and "microbiota" are generally used interchangeably [2, 3]. Microbiomes are by no means new, as the fossil record shows evidence of microbial communities existing over 3.4 billion years ago [4]. Though much research is primarily focused on microbe-metazoan reactions, microbial communities started with simply microbe-microbe interactions that are still persistent today. Some examples include competition for nutrient uptake, secretion of extracellular enzymes,

secretion of antimicrobial peptides, horizontal gene transfer, parasite transfer, quorum sensing, and cross-feeding [5]. These interactions create a dynamic yet homeostatic local community ecosystem, or a 'supra-organism' as some have termed it, and successful microbiomes are resilient to disturbances, such as colonization from invasive pathogens [6, 5].

Microbiomes are resilient as a result of functional diversity and functional redundancy [5]. Whereas diversity can generally be measured by the number of different phyla or genes present, functional diversity involves the range of traits encompassed by the organisms present in an ecosystem, such as the abilities to fix nitrogen, change the local pH, or produce antimicrobial peptides [7]. Functional redundancy, on the other hand, is the redundancy of species able to perform those certain tasks, so if the environment changes and one species suffers trauma or becomes extinct, another can take its job to maintain the health of the ecosystem [5]. Due to the co-dependence of resilience on both functional diversity and redundancy, a balance between the orthogonal qualia evenness and richness benefit community stability [8]. Evenness is a measure of how evenly species are distributed, independent of how many species are present, such that having 10 organisms of species A and 2 organisms of species B would be less even than 5 organisms of species A and 5 organisms of species B, and richness is a measure of how many taxa are present, where having 5 organisms of species A and 5 organisms of species B would be less rich than having 1 organism of species A, B, C, D, and E [7]. Functional evenness, or the evenness of species able to perform certain functions in microbiomes, is positively correlated with community stability, it yields functional redundancy to stabilize the community in the case of trauma [7]. Likewise, functional richness increases the functional diversity of a community [7]. Though the relationship between richness and evenness on a spatial scale has not been fully elucidated in commensal microbiomes, ecological research suggests that on a small spatial scale, richness and evenness are inversely correlated, but when the spatial scale increases the negative relationship vanishes [9]. This is likely related to the functionality of taxa interacting with environmental conditions, as the abundance of certain resources or lack of antagonist factors (such as predators) in one area may lead to increased proliferation of certain taxa over others [9]. Despite the lack of research on the relationship between evenness and richness in commensal microbiomes, research

does demonstrate differences in the alpha diversity in different locations of murine colon [10].

Just as individual microbes in communities interacted with each other via the release and detection of signaling molecules, evolving eukaryotes also interacted with the preexisting microbes in their communities [11]. One main example of this is the incorporation of *Alphaproteobacteria* as mitochondria in almost all known eukaryotic cells [12]. Another is the theory that the innate immune systems of vertebrates evolved as a response to microbiomes [13]. Additionally, interactions between microbial communities and eukaryotes were crucial to the evolution of early vertebrates, and physiological responses to microbiota have been evolutionarily conserved such that all species of vertebrate today exist with multiple microbiomes [14]. *Homo sapiens*, for example, have microbiota identified in locations primarily including but not limited to the skin, vagina, and gastrointestinal tract [15]. These microbiomes, like others found in nature, are dynamically homeostatic: inter-microbiome variation is greater than temporal variation within a single microbiome [16]. Microbiomes in different locations, such as the ear, skin, vagina, and feces, have their own unique signatures, and most microbiomes from the same location are dominated by the same groups of bacteria [17]. However, high inter-microbiome diversity is not limited to microbiomes in different locations on the body, as the variance between in the same location of the microbiome between individuals (e.g. two gut microbiomes in different individuals) is greater than the temporal variance within each of those microbiomes [16]. Due to the consistent and generally temporally undeviating nature of these microbiota, vertebrate physiology has evolved to rely on certain functions of the microbiota. This can be largely evidenced by the significant physiological disruptions - such as altered metabolism, dysfunctional immune systems, increased inflammation, vascular remodeling, and neurological issues - experienced by germ-free vertebrates [18, 19].

1.2 The Human Gut Microbiota

The largest microbiota of *Homo sapiens*, the gastrointestinal, or 'gut', microbiota has a mass equivalent to roughly 2% of the adult body mass, and there are 150 times more unique bacterial genes present in a standard human host microbiota than there are genes present in the human genome [20, 21, 22]. This gut microbiome contains an estimated 10^{14} microbial cells and at least

10^{15} viruses [23, 24]. Like other vertebrates, the human gut microbiota has a very important role in regulating health and disease, and it has been the focus of a large body of research [17]. The gut microbiota is provided resources by undigested food (largely plant fiber) that makes it to the colon, and the microbes break down or alter these fibers to produce metabolites by which they can interact with the host body [25]. A primary metabolite that will be discussed is short chain fatty acids (SCFA).

1.2.1 Development of the Human Gut Microbiota

Though there is controversy around evidence for the subject, a developing human is believed to be exposed to microbes starting as early as fertilization, when egg may be exposed to microbes from the uterine cervix, from the vagina, or from semen, even in the case of in-vitro fertilization [26, 27]. Early microbial exposure from the endometrial microbiome is also believed to affect implantation via the immune system, as inflammatory responses to microbiota will compromise the success of implantation [28, 29, 30]. In theory, the prevention of implantation of a fertilized egg in the case of an inflammatory uterine microbiota may prevent the development of maladapted immune system [27]. Despite the stigma of the sterile womb dogma, evidence that the implanted embryo is exposed to microbes through the placenta and amniotic fluid dates back to 1927 and has been replicated multiple times through both metagenomics-based and non-metagenomics-based methods [27, 31, 32, 33]. The microbiome of the placenta, which ideally contains non-pathogenic microbes, is low in abundance but rich in metabolic diversity, and it exhibits a profile more similar to that of the oral microbiome than to the vaginal microbiome [33]. Other than direct transmission from the vaginal microbiota, there are multiple proposed methods as to how microbes translocate to the placenta, including migration from the gastrointestinal tract and migration from the oral microbiota. Mouse models have shown translocation of bacteria from the gut microbiota to the placenta, and there are mechanisms by which oral microbes and periodontal pathogens may enter the bloodstream and spread to the placenta [34, 35, 36]. Hematogenous spread (through blood) of oral microbes to the placental microbiota may be a potential mechanism by which of periodontitis can impact preterm birth [37]. The effect of

periodontal pathogen translocation does not appear to occur by directly changing the composition of the placental microbiome but by altering the behavior of typically benign microbes to become more pathogen-like [37]. Interestingly, the placental microbiome correlates less with obesity and metabolic factors of the mother than it does with frequency of antenatal infections including lower urinary tract infections, pyelonephritis, and sexually transmitted infections such as *Neisseria gonorrhea* and *Chlamydia trachomatis*, which could be a result both of treatment with antibiotics and the resilience of pathogens [33]. For example, *Escherichia coli*, which is common in both lower urinary tract infections and pyelonephritis, can bind to uroplakins to evade immune detection and therefore remain present within the host body until opportune chances to recolonize arise [38]. Maternal environmental microbial exposure, including exposure to farmland during pregnancy, also modulates the placental microbiome and is recognized as a predictor of health throughout the lifespan [39]. Though research supports a positive correlation infection by pathogenic bacteria with preterm birth, it has been difficult thus far to characterize what a 'healthy' pregnant uterine microbiota should contain due to the existing (yet changing) dogma of the sterile womb and technical and ethical issues of sample collection during pregnancy [27, 40]. Despite the controversy surrounding the concept, it can be concluded that bacteria are present in amniotic fluid without cases of infection or adverse outcomes, and colonization by non-pathogenic bacteria in the placenta can program the fetus's metabolic pathways and immune system through stepwise microbial exposure, making it more resilient against pathogenic microbes that may contribute to adverse outcomes before or shortly after birth and even throughout the lifespan [41].

The first two years of life comprise an incredibly important window of opportunity for colonization and immune modulation, and primarily starting when the newborn is exposed to a large abundance of microbes from the mother's vaginal canal and the environment at birth [36]. Despite theories that lasting colonization of the gut microbiota begins at birth, analyses of microbiota from the meconium, placental, amniotic fluid, and colostrum in mother-infant pairs provide evidence that colonization begins before birth and that placental microbiota may be more influential on the development of the meconium microbiota than the delivery method [39, 42]. However, as a newborn matures, microbial exposure from the vaginal canal, from the

environment, and from food has a larger effect on the gut microbiota than pre-delivery exposure, and the structure of the gut microbiota shifts toward representing that of a fully developed human [41, 43]. At 6 days post-delivery, gut microbiota differences between vaginal and caesarian-section delivery methods are evident. The gut microbiota of vaginally delivered infants resembles that of the mothers vagina, as it was the first exposure to microbes at birth, whereas the gut microbiota of caesarian-section delivered babies more closely resembles the microbiota of the mother's skin and environment [44, 43]. In a newborn's early life, breast milk - especially colostrum - which is rich in diverse oligosaccharides, provides support for bacterial growth within the colon [34]. Human milk oligosaccharides (HMOs) are not degraded by the infant, and their structures are specific to degradation abilities of certain bacteria regarded as being immunoregulatory, such as *Bifidobacterium longus* subsp. *infantis* [34, 45]. Immunoregulatory bacteria can improve stress resilience through the brain-immune axis during the highly stressful period of time around birth via multiple mechanisms including normalization of the interleukin-6 (IL-6) response to stress and increase in regulatory T cell levels [46, 47]. Prebiotics in breast milk also serve an antimicrobial role against certain pathogens such as group B *Streptococcus* and *Candida albicans*, and they protect against pathogen colonization by supporting the development of high levels of microbial richness in a child's microbiota [34]. As the composition of breast milk changes and a child is exposed to new pathogens, the diversity of the gut microbiota increases, yet it retains high abundances of certain colonizing bacteria [43, 34]. Around 2 to 3 years of age, an individual's unique microbial phenotype becomes relatively established, and sequencing methods show that the gut microbiota of healthy children tends to have higher levels of *Bifidobacterium*, certain strains of *Escherichia coli*, *Faeacalibacterium prazsnitzii*, and *Lactobacillus* than the gut microbiota of children with diseases such as infection, necrotizing enterocolitis, diabetes, and inflammatory bowel diseases [34, 48].

As an individual matures and the gut microbiota becomes established, multiple studies have demonstrated that the dominant bacterial species shift from *Actinobacteria* and *Proteobacteria* to *Firmicutes* and *Bacteroidetes* in individuals with low disease burdens [49]. In adulthood, individuals have highly variable microbiota dependent on diet, travel, illness, hormone cycles, and

genetics, though genetics are a lesser influence than the other aforementioned factors, as evidenced by studies demonstrating that identical twins share only 50% of their microbiota [49, 50, 51]. Though a healthy adult microbiota is rich in *Firmicutes* and *Bacteroidetes*, acute and chronic trauma to the microbiota via antibiotic use, poor diet, or chronic stress can alter this balance [51, 52]. This altered balance can include decreasing the abundance of *Bacteroidetes* and *Firmicutes*, decreasing the *Firmicutes* to *Bacteroidetes* ratio, increasing the abundance of *Proteobacteria*, and decreasing the richness of the microbiota [51, 52]. All of the aforementioned changed tend to be associated with chronic inflammatory diseases. Unfortunately, altered gut microbiota associated with poor health, referred to as dysbiosis, creates shifts in host physiology, such as hyperactive stress responses, that perpetuate the dysbiotic state [52]. Dysbiosis, however, should not be characterized using any specific definition based on microbiota diversity or abundances nor as the binary opposite of eubiosis: variability in microbiota are not such that certain characteristics make the host more or less healthy in all areas of the world, disease states, or ages [53]. Thus, referring to dysbiosis as a specific microbial signature detached from specifics such as host health metrics, demographics, and age is misleading, and more appropriate means of alluding to dysbiosis include referring to the microbiota as trending toward known dysbiotic factors (given known host health factors), referring to the microbiota compared to a control (not 'healthy') group with similar characteristics, or a combination of both. Though much research exists regarding dysbiotic states, one must consider its limitations and not overreach into attempting to define globally healthy and unhealthy microbiota or hosts solely based on microbiome data. A key example cited by Brussow is that bottle-fed infants have greater gut microbiota alpha diversity than breast-fed infants, yet this does not translate to greater health outcomes [53, 54].

1.2.2 Host-Microbiota Interactions

Through mechanisms outlined in the Layered Hygiene Hypothesis and the Old Friends Hypothesis, stepwise exposure to microbes throughout the first few years of life affects disease risk throughout the lifespan via exposure to immunoregulatory microbes and establishment of certain

microbial phenotypes that affect pathogen colonization and stress resilience [55, 56, 57]. Inflammation associated with the immune activation that can be triggered by the gut microbiota plays multiple roles in various diseases including but not limited to inflammatory bowel disorders, metabolic syndrome, and psychiatric disorders [58, 59, 60, 61]. There are multiple mechanisms by which this occur, such as through antigen exposure, gene exposure, and peptide production, but one primary mechanism is the fermentation of dietary fibers to produce short chain fatty acids (SCFAs) ranging from 2 to 6 carbons in length [62].

1.2.2.1 Fibers: from the host to the microbiota

Since the human digestive system only produces roughly 17 gastrointestinal enzymes, and carbohydrates can only be absorbed as monosaccharides at the brush border of the small intestine through SGLT1 and GLUT5 transporters, many plant fibers and lignins with complex structures completely or partially escape digestion [63, 64, 65]. These complex plant fibers are defined as dietary fibers by the *CODEX Alimentarius Commission* as carbohydrates with lengths over 10 monomeric units that are not hydrolyzed by the enzymes endogenously present in the small intestines of humans. Some definitions of dietary fibers, such as those by the Australian, Canadian, and New Zealand food standards and public health groups include carbohydrates as short as 3 monomers in length [65, 66]. The overarching concept of dietary fibers is that they are not digested by the endogenously produced human enzymes by the time they leave the small intestine, and there are many types of dietary fibers that vary based on the species of plant from which they originate [67, 65]. Most dietary fibers are prebiotics, or particles that are resistant to gastric acid in the stomach and hydrolysis in the small intestine and that are fermented by the gut microbiota, stimulating the growth of non-pathogenic bacteria; however, not all dietary fibers are prebiotics, and not all prebiotics are dietary fibers [65]. Dietary fibers can be categorized into soluble and insoluble fibers based on their solubility in water, and these fibers can have laxative or constipating effects based on their structures and viscosity (if soluble) [67]. Different ratios and abundances of each type of dietary fiber can effect the composition of the microbiota by modulating the amount of time that resources are available in the colon and the frequency by

which microbes are removed from the colon during luminal washout [67, 68, 69]. Insoluble fibers with large, course particle sizes irritate the gut mucosa, causing a laxative effect, whereas viscous soluble fibers slow gut transit and help to normalize stool consistency [67]. Fast colonic transit is associated with higher abundances of bacterial species such as *F. prausnitzii* that are associated with a healthy mucosal barrier and decreased low-grade inflammation, and slow colonic transit is associated with a more methanogenic profile, higher bacterial protein catabolism, increased mucosal degradation by bacteria, and other factors trending toward dysbiotic factors [69]. However, stool transit being too fast will result in increased flushing of microbes and potential disruption of the microbial environment, insoluble fibers are poorly fermented by the microbiota, and viscous soluble fibers have non-microbiota-mediated health benefits, such as trapping bile, which lowers cholesterol levels, so it is important to have a balance of soluble and insoluble fibers [67, 70, 71]. Non-viscous soluble fibers, such as resistant starches, which are long strains of amylose-like digestible carbohydrate that cannot be fully degraded in the small intestine due to a lack of time rather than a lack of enzyme functionality, function as rapidly fermentable prebiotics for the microbiota [67].

1.2.2.2 Short chain fatty acids: from the microbiota to the host

Once dietary fibers and resistant starches reach the colon, they are fermented by bacteria to produce SCFAs including acetic acid, propionic acid, butyric acid, valeric acid, and caproic acid [72]. Branch-chain isomers of SCFA (BSCFA) including isobutyric acid, 2-methyl butyric acid, and isocaproic acid are not produced by fiber fermentation. Instead, they are products of bacterial metabolism of valine, leucine, and isoleucine [72]. These acids are assumed to be in the deprotonated form in the colon and are therefore referred to with the -ate suffix (e.g. butyrate). In healthy individuals, acetate, propionate, and butyrate constitute 95% of the SCFAs produced, and they are produced in a ratio of 60:20:20, respectively [62, 73]. The general stoichiometry for the fermentation of carbohydrate to produce SCFA is 59 $C_6H_{12}O_6$ + 38 $H_2O \rightarrow$ 60 CH_3COOH + 22 CH_3CH_2COOH + 18$CH_3CH_2CH_2COOH$ + 96 CO_2 + 268 H^+ + heat + additional bacteria [74]. Roughly 95% of SCFAs produced are absorbed, and they make up almost 10% of the energy

requirements of humans [62]. Though only about 5% of the SCFA produced are excreted, SCFA research has focused on fecal SCFAs due to the impracticality of measuring colonic SCFAs [76]. Findings suggest that fecal SCFA ratios - but not the amounts passed in the feces due to varying SCFA absorption rates between individuals - are representative of colonic production, and ratios between the SCFAs correlate with health and disease states [75, 76]. SCFAs decrease the luminal pH of the colon, decreasing the solubility of bile salts, increasing mineral absorption, and altering the microbiota, inhibiting pathogen growth [77, 78].

As acetate is able to escape metabolism in the liver, it makes up the highest proportion of SCFA in systemic circulation, though there are multiple factors confounding this data, such as the endogenous production of acetate [72, 77]. Outside of microbiota research, acetate is known as a source for central carbohydrate metabolism when nutrients are limited, and it is used as a parallel pathway for acetyl CoA production [79]. Additionally, emerging research suggests that the *de novo* source of acetate in mammals is from conversion of pyruvate via coupling to reactive oxygen species and via the activity of alpha-keto dehydrogenases [79]. Acetate is produced from the fermentation of acetogenic fibers such as inulin and galacto-ligosaccharides primarily in the proximal colon, but it can also be produced by fermentation of peptides and fats in the distal colon [80]. Due to acetate's ability to be produced by the fermentation of fats and nitrogenous compounds, fecal and serum acetate percentages are increased by high fat diets (HFDs) [80]. Higher acetate production is associated with an increased *Firmicutes*/*Bacteroidetes* ratio, which tends to correlate with a dysbiotic state and negative health outcomes [80, 81]. Through increased parasympathetic activity mediated by the vagus nerve, acetate increases glucose-stimulated insulin secretion via the microbiota-β-cell axis, and it triggers the release of ghrelin, a peptide that regulates appetite (among other roles) and is commonly referred to as the 'hunger hormone' [81, 82]. The combination of these two promotes metabolic syndrome by promoting hyperphagia (increased hunger from ghrelin), hypertriglyceridemia, and increased fat storage [81, 82]. Long term upregulation of insulin secretion due to acetate is thought to contribute to insulin resistance and metabolic syndrome [77]. Due to its ability to be converted to Acetyl-CoA, acetate can promote cholesterol synthesis and lipogenesis [77, 83]. 50-70% of acetate is metabolized in the

liver, where it can contribute to non-alcoholic fatty liver disease (NALFD) in the case of elevated acetate levels, and the rest is oxidized by muscle tissue [77, 84, 85]. Acetate is also produced by acetogens that can consume H_2 for energy and release methane, acetate, and H_2S as end products, increasing the ability of NADH to be reoxidized to NAD^+ [86]. Primary fermentation is generally limited by the buildup of H_2 and reducing equivalents inhibiting reoxidation of NADH, so acetogens increase the efficiency of fermentation by consuming H_2 [87]. Decreased inhibition of primary fermentation leads to increased SCFA production and therefore increased energy contribution to the host, promoting obesity [86].

Unlike acetate, propionate is unable to bypass the liver, so it thus makes up a lower proportion of the SCFA in circulation [72]. Propionate in the liver is used for gluconeogenesis, and it inhibits hepatic lipogenesis and cholesterol synthesis via inhibiting HMG CoA reductase [77, 72, 88]. Propionate can trigger intestinal gluconeogenesis through a mechanism dependent on G protein-coupled receptor GRP41 and through the gut-brain axis [89, 90]. Propionate is produced through the fixation of CO_2 to form succinate and from lactate and acrylate via the acrylate pathway, and it it incredibly important for gluconeogenesis in ruminants [77]. On the grounds of immunomodulation, propionate can trigger increased extra-thymic *de novo* production and differentiation of T_{reg} cells, which has an anti-inflammatory and anti-metabolic syndrome effect via regulating the T_H1/T_H2 ratio in the body and other immunosuppressive measures [91, 92, 93]. T_{reg} cells play an important role in staving the pathogenesis of autoimmune disorders and allergies in addition to gut disorders, such as inflammatory bowel disease, Crohn's disease, and ulcerative colitis, suggesting a role of propionate in preventing gastrointestinal disorders, especially those linked to eosinophilic and autoimmune reactions [94, 95]. Another suspected mechanism for immunosuppression by propionate (as well as butyrate) is its ability to bind to GPR41 and GPR43 which are common in mammalian immune cells, but specific anti- or pro-inflammatory effects of these receptors are not well understood [96, 97]. Propionate, in a pH under 5, can kill pathogenic *E. coli* and *Salmonella*, protecting the epithelium from colonization [98]. Another means by which propionate protects the gut epithelial border is by supporting apoptosis of colonocytes [75].

Butyrate serves as the major substrate for energy production in the ceco-colonic epithelium, and a lack of butyrate leads to autophagy due to increased intermediary metabolism, not solely due to its role as a histone deacetylase (HDAC) inhibitor as previously thought [77, 85, 99]. The colonic epithelium is highly influenced by butyrate, as its absence triggers rapid and overactive autophagy, and abundance triggers apoptosis of tumor cell lines [75]. Additionally, butyrate inhibits tumor necrosis factor-α and interleukin 13 to affect the expression of proteins that regulate structure of colonocyte tight junctions [100]. Poor tight junction structural integrity is thought to lead to intestinal permeability, immune hyperactivation, chronic inflammation, and risk of metabolic diseases [101]. The mammalian gut exists in a state of relative hypoxia, and the microbial production of butyrate decreases colonocyte oxygen consumption, stabilizing the transcription factor hypoxia-induced factor-1 (HIF-1), which performs epithelial barrier-enhancing functions, again protecting against colitis and chronic diseases [102]. Butyrate inhibits the production of nuclear factor kappa-B (NF-kB), which is highly active in regulating systemic production of inflammatory cytokines that are active in the immune-brain axis and the development of major depressive disorder [103, 104].

Other SCFA are not as well studied as acetate, propionate, and butyrate, but they are still relevant to health maintenance. Valerate (also referred to as pentanoate), like butyrate, suppresses autoimmune pathologies by inhibiting HDAC and therefore downregulating IL-17 production in $CD4^{+}$T lymphocytes [105]. Valerate, unlike butyrate, does not alter the production of T_{reg} cells, demonstrating different mechanisms of action in immunosuppression between them [105]. In mouse studies, valerate has shown to mediate regulatory B cells protecting against autoimmune disorders [105]. Valerate has also demonstrated ability to impair growth of *Clostridioides difficile* and *E. coli* in the gut [106, 107]. Increased valerate and caproate levels are associated with increased richness and high abundances of *Prevotella* and *Coprococcus* [108].

1.3 Microbiome Analysis

Since a large fraction of bacteria present in the microbiota have yet to be reliably cultured successfully, microbiomes are primarily analyzed via sequencing of the RNA present in the feces

[109]. The 16S ribosomal RNA subunit appears to be conserved across most bacterial species, so it has become useful tool to analyze a representation a microbiota sample's structure [110, 111]. However, the so 16S rRNA subunit is too long (1400 base pairs) to be sequenced in one read with the current technology available in a cost-efficient manner, but it can be broken into hyperconserved and hypervariable regions that are short enough to be read by systems such as Illumina's HiSeq and MiSeq (capable of less than 250 base pairs at a time) [112, 113]. The conserved regions can be used as 'anchors' to denote the loci of 8 variable regions, allowing for sequencing of variable regions to create identifiers for different taxa present in the sample[112]. Polymerase chain reaction primers can be designed based on the conserved regions to sequence specific variable regions via next-generation sequencing [112]. However, based on different variability seen in certain variable regions of specific microbiomes, some variable regions are better suited for analyzing certain microbiomes, such as gut or soil though using these variable regions may promote specific biases, shifting the observed taxa to misrepresent what is actually present [114, 113]. More variable regions can be sequenced to provide higher accuracy, but the cost, time, and computational resources increase with the number of base pairs sequenced, so one must acknowledge the trade off made between cost and accuracy (including the inherent biases present based on variable region sequenced) [115, 116]. Though researchers with more resources may use more variable regions, sequencing the V4 variable region via 515f/806r primers per the Earth Microbiome Project 16s Illumina Amplicon Protocol has emerged as a popular and standardized approach across various projects including the American Gut Project, the Human Microbiome Project, the Flemish Gut Flora Project, and the Sponge Microbiome Project
[17, 117, 118, 119, 120].

1.3.1 Using QIIME2 for Microbiome Analysis

Data generated from 16s sequencing is large and complex, and it must be analyzed using computational methods. One program used to do so is Quantitative Insights Into Microbial Ecology 2 (QIIME2), a decentralized and open-source microbiome analysis software package that allows for transparency via data provenance tracking [121]. A typical workflow in QIIME2

involves demultiplexing sequences, removing likely misreads (or 'noisy' sequences), and dereplicating sequence reads (while maintaining a count of sequences present) to decrease the amount of data that must be to processed [121, 122]. The QIIME2 denoising plugins DADA2 and Deblur check for chimeras, such as mitochondrial rRNA sequences that might pollute samples, and they cluster similar sequences into operational taxonomic units (OTUs) with their frequencies stored in feature tables [122, 123, 121]. Once OTUs are generated, they can be assigned taxonomy by a machine learning classifier (such as a Naïve Bayes classifier) trained on 16s databases, such as SILVA or GreenGenes [124]. Naïve Bayes classifiers have shown reliable efficacy for assigning taxonomy, and they are based off Bayes' Theorem for conditional probability stating the following:

$$P_{(A|B)} = \frac{P_{(B|A)} \times P_A}{P_B}$$

In this equation, P_A represents the probability of a certain taxonomic classification being true, and P_B represents the probability of the sequence data being true. A Naïve Bayes classifier will identify the most likely taxonomic classification, given the sequence data and database provided. Additionally, QIIME2 plugins create a pipeline for aligning sequences and for generating rooted and unrooted phylogenetic trees that can be visualized or used for diversity analyses [125]. Diversity analyses in QIIME2 can be run individually through a core diversity pipeline, and multiple measures of alpha and beta diversity can be tested, and emperor plots can be generated to demonstrate differences in microbial communities [121]. QIIME2 also includes a variety of other more specialized plugins such as supervised and unsupervised machine learning sample classifiers that have successfully predicted cancer and wine quality [126, 127].

1.3.2 Diversity Measures

Understanding the diversity measures clarifies the information provided to the researchers and the limitations of each measurement. Alpha diversity, or the diversity within a sample, is commonly measured using Shannon's diversity, observed OTUs, Faith's Phylogenetic diversity, and Pielou's Evenness. Common measures of beta diversity, which is the diversity between

samples, include Jaccard, Bray-Curtis, unweighted UniFrac, and weighted UniFrac. Diversity measures can be classified as phylogenetic/nonphylogenetic and qualitative/quantitative. Qualitative measures of diversity simply focus on the number of different taxa focused, whereas quantitative measures place weight on the number of each taxa present.

1.3.3 Alpha Diversity

Observed OTUs is the easiest to calculate, as it, a nonphylogenetic, qualitative measure, is simply a total of the number of OTUs present in a sample. Shannon's diversity index (H), which is quantitative and nonphylogenetic, is calculated as:

$$H = -\sum_{i=1}^{S} p_i ln(p_i)$$

Here, p_i is the proportion of population the population constituted by OTU i, and S is the total number of OTUs present [128]. Faith's phylogenetic diversity is phylogenetic and qualitative, and it is the sum of all the lengths of the branches of the phylogenetic tree for a community [129]. Pielou's evenness (J') is not a measure of richness but a measure of evenness [130]. It can be calculated as:

$$J' = \frac{H'}{H'_{max}}$$

Here, H'_{max} is the max possible value of Shannon's diversity index for the given population (which assumes only one organism per species S, so $P_i = \frac{1}{S}$) and can be calculated as:

$$H'_{max} = -\sum_{i=1}^{S} \frac{1}{S} ln\left(\frac{1}{S}\right) \tag{1}$$

$$H'_{max} = -S\left(\frac{1}{S} ln\left(\frac{1}{S}\right)\right) \tag{2}$$

$$H'_{max} = -ln(S^{-1}) \tag{3}$$

$$H'_{max} = ln(S) \tag{4}$$

Thus:

$$J' = \frac{H'}{ln(S)}$$

1.3.4 Beta Diversity

Jaccard distance is a nonphylogenetic qualitative measure of community similarity, and it can be written as:

$$J_{A,B} = (A \cap B)/(A \cup B)$$

Here, A is one sampled community, and B is another sampled community, such that the Jaccard distance is the number common OTUs divided by the total number of OTUs in observed in the two samples [131]. Bray-Curtis distance is a nonphylogenetic quantitative measure of community dissimilarity, where the dissimilarity D between samples A and B is:

$$D_{A,B} = \frac{\sum_{i=1}^{S} |n_{Ai} - n_{Bi}|}{n_{A+} + n_{B+}}$$

Here, n_{Ai} is the abundance of OTU i in sample A, and n_{A+} is the total of all species abundances in sample A [132, 133]. As Bray-Curtis is the difference in species abundances divided by the total abundances, it is limited by the assumption that both samples contain a similar abundance and occupy a similar physical area or volume [132]. UniFrac distances are used to analyze phylogenetic differences between two samples [134]. Unweighted UniFrac is qualitative and thus does not place 'weight' on the abundance of each taxa present, and it (u) for communities A and B can be calculated as:

$$u_{A,B} = \sum_{i=1}^{S} \frac{b_i}{b_t} \quad \ni i = A \triangle B, t = A \cup B$$

In this equation, b_i is the length of branch i that is not shared in communities A and B, and b_t is the length of all branches in A and B individually [134]. To calculate a raw weighted UniFrac

value (w) for communities A and B:

$$w_{A,B} = \sum_{i}^{S} b_i \times \left| \frac{A_i}{A_t} - \frac{B_i}{B_t} \right|$$

In this equation, n represents the number of branches, and b_i is the length of branch i. A_i represents the abundance of OTUs descending from each branch i in community A, and it is divided by A_t,the total abundance of sequences in community A in order to balance out unequal sampling [135]. In cases with rapidly evolving taxa, where branch lengths might be highly variable, branch length is replaced with the sum of the length of the branches from the root to further normalize branch length values [135].

2 Methods

2.1 Patient Recruitment

Patients (n=20) were recruited through the process outlined in Webb 2019 [136]. Inclusion criteria for patients included the presence of predefined gastrointestinal symptoms at least three times per week, self-identification as healthy, and age over 18 years. Exclusion criteria included diagnosis of celiac disease, irritable bowel disorder, inflammatory bowel disease (including Crohn's disease and ulcerative colitis); current consumption of prebiotics, probiotics, enzymes, non-steroidal anti-inflammatory drugs (NSAIDs), fish oil, and/or fiber supplementation unless willing to cease supplementation 2 weeks prior to the study; prescribed use of any NSAID; and pregnancy or intent to become pregnant within 60 days. Before commencing the study, all participants were administered an informed consent document. A subset of the participants (n=11) was used for microbiome analysis. This study was fully approved by the ETSU Institutional Review Board on December 5, 2017; study number 1117.22f.

2.2 Study Design

This study was split, partially blinded, and placebo-controlled. Participants were split into two groups, A and B, by a random number generator. Both groups went through a two-week washout period, and for the second four weeks (28 days) group A was assigned to take the Glutenshield supplement 3x daily with meals while group B was assigned to take a placebo 3x daily with meals. Participants were not informed whether they were given the placebo or control supplement. Following the two week washout, on day 0 of the active portion of the study, participants arrived with a stool sample collected 'at home', and two tubes of whole blood were drawn. Participants completed a survey of gastrointestinal symptoms, and they were given a bottle of 84 Glutenshield or Placebo pills, dependent upon their assigned group. On day 28 of the active study, participants returned with a stool sample collected 'at home', gave another blood sample of equal volume, and filled out the gastrointestinal symptoms questionnaire.

2.3 Supplement Contents

The placebo supplement was a 1:1 mixture (by mass) of microcrystalline cellulose (Avicel) and bentonite powder. Glutenshield is a synbiotic supplement developed by Shield Nutraceuticals. It contains the probiotics *Lactobacillus acidophilus*, *Lactobacillus casei*, *Lactobacillus rhamnosus*, *Lactobacillus plantarum*, *Lactobacillus brevis*, *Lactobacillus salivarius*, *Lactobacillus coagulans*, *Bifidobacterium lactis*, *Streptococcus thermophilus*, *Bifidobacterium bifidum*, *Saccharomyces bouldarii*; the prebiotics chitosan oligosaccharide, fructooligosaccharide, alfalfa, *Emblica officinalis* extract, papaya juice powder, fulvic acid, and ionic minerals; and the enzymes dipeptidyl peptidase IV, lactase, cellulase, hemicellulase, xylanase, phytase, serrapeptase, and plant-based lipase, protease, and amylase. Both supplements were encapsulated by Vcaps Enteric capsules.

2.4 GI Symptom Questionnaire

The GI symptom questionnaire completed on days 0 and 29 included a Likert numerical scale that ranged from 1 to 7, with 1 being no symptoms and 7 being constant/severe symptoms, and

participants were instructed to fill it out based on their symptoms over the past week. The symptoms indicated on the questionnaire included abdominal pain/ discomfort, heartburn, acid regurgitation, bloating, nausea and vomiting, abdominal distension, eructation (burping), increased gas, decreased passage of stools, increased passage of stools (rapid transit), loose stools, hard stools, urgent need for defecation, and feeling of incomplete evacuation.

2.5 Blood Sample Collection and Analysis

On day 0 and day 29, 10mL blood samples were collected in two 8.5 mL Becton Dickinson vacutainers. Following collection, the samples were put on ice and brought to ETSU's health science laboratory, where they were allowed to clot at room temperature for 30 minutes and then centrifuged at 3000 x g for 10 minutes. After centrifugation, 1 mL of serum supernatant was transferred to a 1.5 mL polypropylene Fisherbrand micro-centrifuge tube via Eppendorf pipette, and 2 mL of serum supernatant was transferred to a Fisher Scientific amber vial via Eppendorf pipette, and the transferred serum was stored at -80°C until needed for analysis. Analysis of serum was performed using commercially available ELISA plates from Aviscera Bioscience. ELISAs were performed to test for IgG1, IgG2, IgG3, IgG4, IgA, IgM, IL-2, IL-6, IL-8, and TNF-α.

2.6 Fecal Sample Collection and Analysis

Upon completion of the informed consent, participants were given multiple sets of supplies and instructed on how to collect the stool sample using saran wrap placed under the toilet seat. Samples were to be collected within 24 hours of sample submission (days 0 and 24) and stored in a freezer in a self-sealing plastic bag. Stool samples were stored on ice in biohazard containers and transported to ETSU's Nutrition and Dietetics Research Laboratory on the Valleybrook campus. 1 gram of fresh sample was separated and stored at -80°C for microbiome analysis, and the remainder was freeze-dried and ground to be used for nutrient and SCFA analysis. Freeze-drying was performed at 0.077mBar and -50°C for 48-72 hours until samples were thoroughly dry.

2.6.1 Kjeldahl Digestion

Total nitrogen was determined for freeze-dried and ground samples using kjeldahl digestion. For the procedure, 100 mg of the sample was weighed (weight was recorded) into a 100 mL kjeldahl flask along with 1.9 grams of potassium sulfate (K_2SO_4), 80 mg of mercuric oxide (HgO), 2 mL of concentrated (10N) sulfuric acid, and 2 porous boiling chips. The sample was placed on LABCONCO heat mantle. The air was turned on and the mantle was turned to heat setting 3. The sample refluxed for 8-12 hours, the heat mantle was then turned off, and the sample was cooled to room temperature. 15 mL of deionized distilled water (DDW) was added to the kjeldahl flask. The sample was brought to a boil and was filtered while hot into a 150 mL Erlenmeyer flask using P5 grade Fisher brand qualitative grade plain filter paper circles. Following digestion of the samples, distillation was performed to determine total nitrogen per sample. The LABCONCO rapid distillation unit was turned on, set to heat setting of 6-7, and was allowed to heat up. 5mL of 4% Boric acid and a few drops of kjeldahl indicator were added to a new 150 mL Erlenmeyer flask. The flask was placed at the bottom of the distillation unit. The distillate (filtered sample) was added to the top of the unit and the Erlenmeyer flask was rinsed with DDW. The material was emptied into the reaction tube. 10 mL of sodium thiosulfate (NaOH/ $Na_2O_3S_2$) was added to the top of the apparatus and was slowly emptied into the reaction tube. The sample was allowed to distill for 15-20 minutes until the total volume of the boric acid and ammonium solution reached 25-30 mL. During the distillation process, ammonium (NH_4^+) was converted to ammonia gas (NH_3^+). NH_3^+ condensed into the boric acid solution to form ammonium borate. The ammonium borate was then titrated with 0.1 N HCl until a color change was observed (blue $\rightarrow$ red; base $\rightarrow$ acid). The mL of HCl needed to titrate the solution back to an acid was recorded. Nitrogen per kilogram of sample and percent total protein were then calculated. Samples were run in duplicate per participant fecal sample provided.

2.6.2 Fiber Analysis

Total dietary fiber (TDF), soluble dietary fiber (SDF), and insoluble dietary fiber (IDF) was assessed on freeze-dried, ground stool samples using the automated ANKOM Dietary Fiber

Analyzer method AOAC 991.43. Reagants included 78% Ethanol by volume, α-amylase (5mL/25mL DDW), protease (5mL/25mL DDW), amyloglucosidase (5mL/25mL DDW), MES-TRIS buffer, and 0.561N HCl. The MES-TRIS solution was prepared by dissolving 9.76 g of 2-(N-Morpholino)ethanosulfonic acid (MES) and 6.1 g of Tris(hydroxymethyl)aminomethane (TRIS) in 850 mL of DDW and adjusting the pH to 8.2 using 6N NaOH and dilute to 1 L with DDW.

ANKOM IDF and SDF filter bags were labeled with a permanent marker. Each bag was weighed using the Bag Weigh Holder and an AL54 Mettler Toledo analytical balance. The tare bag weight was recorded onto a Dietary Fiber Data Spreadsheet (DFDS). One gram of Diatomaceous Earth was weighed into two separate dishes. The weight of each was recorded onto the DFDS. 0.5$\pm$0.05 g of the freeze dried, ground stool sample was weighed in duplicate into two dishes. The weight of each was recorded onto the DFDS. All fluid levels were checked on the DF analyzer. The instrument and Nitrogen gas were turned on. SDF bags and Clamp Bar D were installed on the instrument. Clamp Bar D was closed and the pre-weighed DE was added to each SDF bag and was rinsed with 2-3mL of DI water. IDF bags and Clamp Bars B and C were installed onto the instrument. Clamp Bar B was closed, pinching off the bags, and the pre-weighed samples were transferred to the IDF bags. SDF bags were hooked to Clamp Bar C. Clamp Bar A was installed. The instrument was started, beginning the automated process of digesting the sample. After the amylase and protease phases, the pH of the samples was checked and adjusted to 4.0-4.7 as needed with 0.561N HCl. After the automated process was complete, IDF and SDF bags were rinsed with Acetone using the ANKOM Acetone Rinse Stand. After drying, the bags were sealed at a heat setting of 3 using the ANKOM Heat Sealer. Samples were placed on a drying rack and were placed in a Fisher Scientific Isotemp oven at 100°C for 90 minutes. Samples were removed from the oven and immediately placed in an ANKOM MoistureStop weigh pouch (desiccant pouch) to cool. Bags were removed one at a time from the desiccant pouch and were weighed on an analytical scale using the Bag Weigh Holder. Bag weights were recorded on the DFDS. A protein correction was performed using kjeldahl digestion and distillation, as described above. An ash correction was also performed by burning the samples as 700°C for 5 hours and

recording the weight after ashing. All ashing and protein values were recorded on the DFDS. Percent IDF, SDF and TDF were then calculated using the following equations:

$$\%\text{IDF or }\%\text{SDF} = \frac{\text{Total residue} - (\text{protein residue} + \text{bag}) - (\text{ash residue} + \text{bag})}{\text{original sample weight} \times 100\%}$$

$$\text{TDF} = \%\text{IDF} + \%\text{SDF}$$

2.6.3 SCFA Extraction and Analysis

SCFA extractions were performed using a procedure developed by Schwiertz et al. that was modified [137]. One mL of the SCFA extraction solution, containing Oxalic acid (0.1 mol/L), Sodium Azide (40 mmol/L), and Caproic acid (0.1 mmol/L)(internal standard) was added to 80 mg of a freeze-dried stool sample in a 16 x 100 mm disposable culture tube. The tube was capped and vortexed for 30 seconds. The tube was placed on a horizontal shaker for 1 hour. The tube was centrifuged at 4000 rpm for 20 minutes. After centrifuging, the supernatant was removed and placed in a 1.5mL polypropylene Fisherbrand micro-centrifuge tube. The solution was re-centrifuged at 12,000 rpm for 15 minutes. Again, the supernatant was removed and placed in a new 1.5 mL micro-centrifuge tube. The solution was re-centrifuged at 12,000 rpm for 15 minutes. Finally, the supernatant was removed, placed in a 2 mL amber vial, and was stored at -80°C until being analyzed using a Shimadzu GC2010 gas chromatograph with SigmaAldrich ZB-Wax Plus capillary column. Samples were run using a method adapted from Schaefer et al [138]. The method included injecting 1 μL of solution with an SPL1 temperature of 250°C. The initial column temperature was 50°C, held for 2 minutes, which rose at a rate of 15 degrees/minute until reaching 140°C with a hold of 5 minutes, followed by a rise at rate of 10 degrees/minute until reaching 160°C with a hold of 3 minutes and a rise of 10 degrees/minute until reaching 175°C with a hold of 3 minutes. The flame ionization detector temperature was 180°C, and the end time of the run was 24 minutes. Samples were run in duplicate, and values for each participant were averaged.

2.7 Microbiome Analysis

2.7.1 16s RNA Isolation and Sequencing

Microbiome analysis was performed on 11 participants in duplicate before and after intervention for a total of 44 samples sequenced and analyzed. Powersoil DNA isolation kit was used to isolate DNA from the portion of the fecal samples stored at -80°C. 250 mg of the sample was added to the Qiagen-supplied PowerBead tube and vortexed. 60 μL of solution C1 (Qiagen lysing agent) was added, the tube was briefly vortexed manually, and then the tubes were secured to an adapter to be vortexed at maximum speed for 10 minutes. The tubes were then centrifuged at 1000 x g for 30 seconds, and the supernatant was transferred to a 2 mL collection tube. 250 μL of solution C2 (Qiagen precipitating agent) was added to the collection tubes, which were then vortexed for 5 seconds and then incubated on ice for 5 minutes. Tubes were then centrifuged for 60 seconds at 10,000 x g, and 750 μL of supernatant was transferred to clean 2 mL collection tubes. 200 μL of solution C3 (Qiagen precipitating agent) was added, and the tubes were briefly vortexed manually and incubated on ice for 5 minutes again. Following incubation, the tubes were centrifuged at 10,000 x g for 60 seconds, 750 mL of supernatant was added to 2 mL collection tubes, 1200 μL solution C4 was added, and tubes were vortexed for 5 seconds. 675 μL of this solution was loaded into a Qiagen kit spin column and centrifuged at 10,000 x g for one minute three times with flow through being discarded between centrifugations. 500 μL of solution C5 was added to the spin column, which was centrifuged at 10,000 x g for 30 seconds and one minute with flow through discarded between centrifugations. The spin columns were placed into clean 2 mL collection tubes, 100 μL nuclease-free water was added to the center of the spin column's white filter membranes, and the samples were allowed to incubate at room temp for 5 minutes. Tubes were centrifuged for 30 seconds at 10,000 x g to elute the DNA, spin columns were discarded, and samples were checked for DNA quantification with a Qubit fluorometric quantification meter on the broad range detection setting. DNA was fragmented and tagged with a 615f/806r adapted sequence before polymerase chain reaction amplification. Samples were sequenced using Nextera MiSeq, and sequences were obtained from Illumina and Swift Biosciences.

2.7.2 Microbiome Analysis

Microbiome bioinformatics analysis was performed with QIIME2 2020.2 [121]. Sequences were imported and demultiplexed utilizing the Import as Casava option of q2-demux. The resulting sequences were denoised, chimera-sorted via consensus chimera sorting, and clutered into OTUs at 97% similarity using q2-DADA2 [139]. Sequences were aligned, and a phylogeny was created using q2-phylogeny [140, 141, 142]. Alpha and beta diversity analyses were performed using the core diversity pipeline of q2-diversity after samples were rarefied to 23,600 sequences per sample [143, 144, 145, 146, 147, 148]. Alpha diversity statistical significance was tested via Spearman's correlation for numerical metadata and Kruskal-Wallis ANOVA for categorical data [129, 149, 150, 151, 152, 130, 128]. A mantel test was used to analyze beta diversity differences between samples' distance matrices, and statistical significance was tested via Spearman's correlation for numerical metadata and PERMANOVA for categorical data [153, 154, 155, 156, 134, 135, 131, 133]. Visualizations and Principle Coordinate Analysis plots were generated via the q2-diversity plugin [157, 158, 159, 160]. Taxonomy was assigned via the q2-feature-classifier plugin using a naïve Bayes classifier trained on the Silva 132 99% OTUs 515F/806R supplied by QIIME2 [161, 162, 163, 164, 165]. q2-composition plugin was used to collapse the feature table for an analysis of community of microbiomes (ANCOM) test to detect differential abundances in different BMI categories and the treatment groups before and after supplementation [166, 167].

3 Results

3.1 Alpha Diversity

3.1.1 BMI

Alpha diversity metrics differences were not statistically significant ($p > 0.05$) between BMI classification groups normal vs overweight, normal vs obese, normal vs overweight + obese (Figure 1).

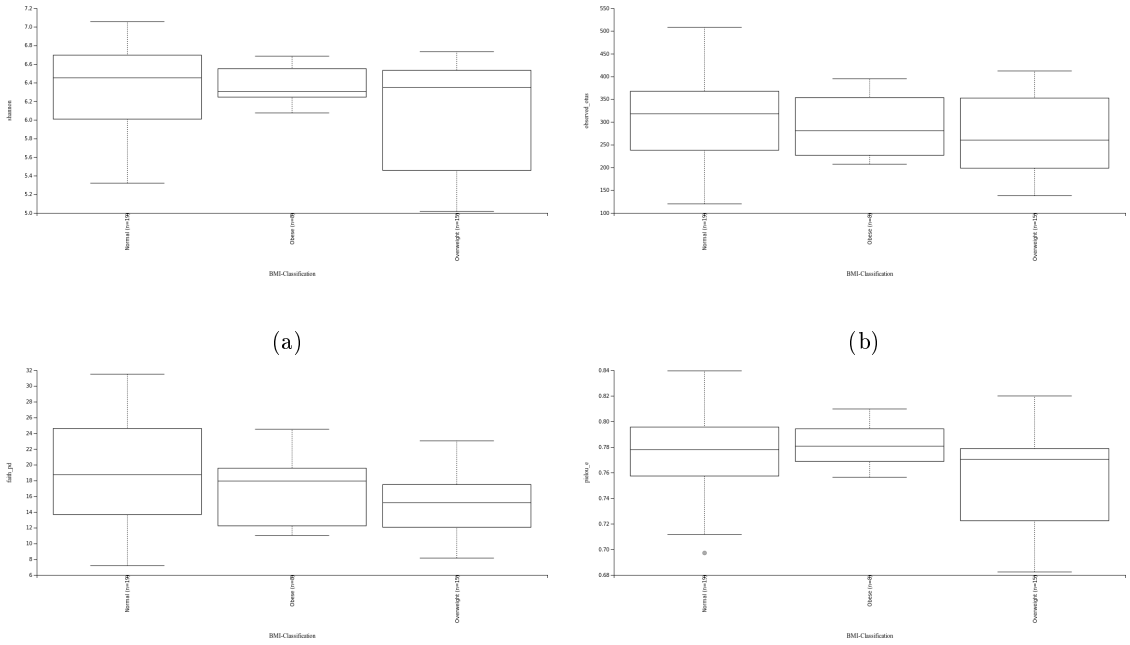

(a) (b)

(c) (d)

Figure 1: BMI Classification (x-axes) plotted against y-axes Shannon's diversity (a), Observed OTUs (b), Faith's phylogenetic diversity (c), and Pielou's evenness (d). Full-size figures can be found in Figures 21-24 of the appendix.

3.1.2 Intervention

Alpha diversity did not significantly change over the course of the study for both the placebo and experimental groups. Interestingly, there were significant differences in alpha diversity metrics between the placebo and experimental groups, independent of the effects of Glutenshield supplementation (Faith p=0.000032, Observed OTUs p=0.0000018, Shannon p=0.000094). Pielou's Evenness was not significantly different between any groups ($p > 0.05$) (Figure 2-5).

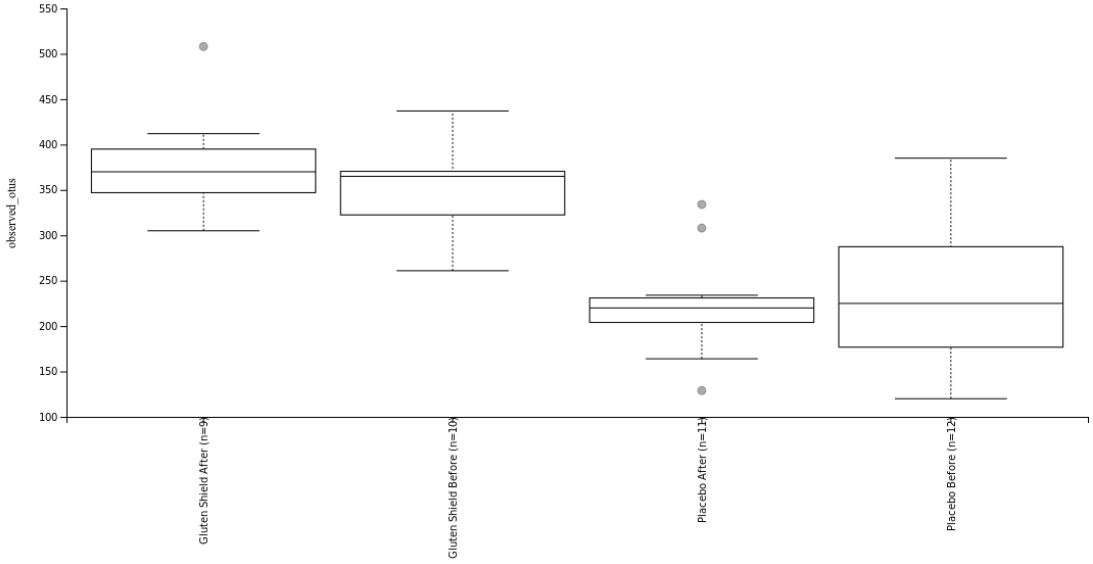

Figure 2: Observed OTUs (y-axis) for experimental and control groups before and after Glutenshield supplementation. Dots represent statistical outliers.

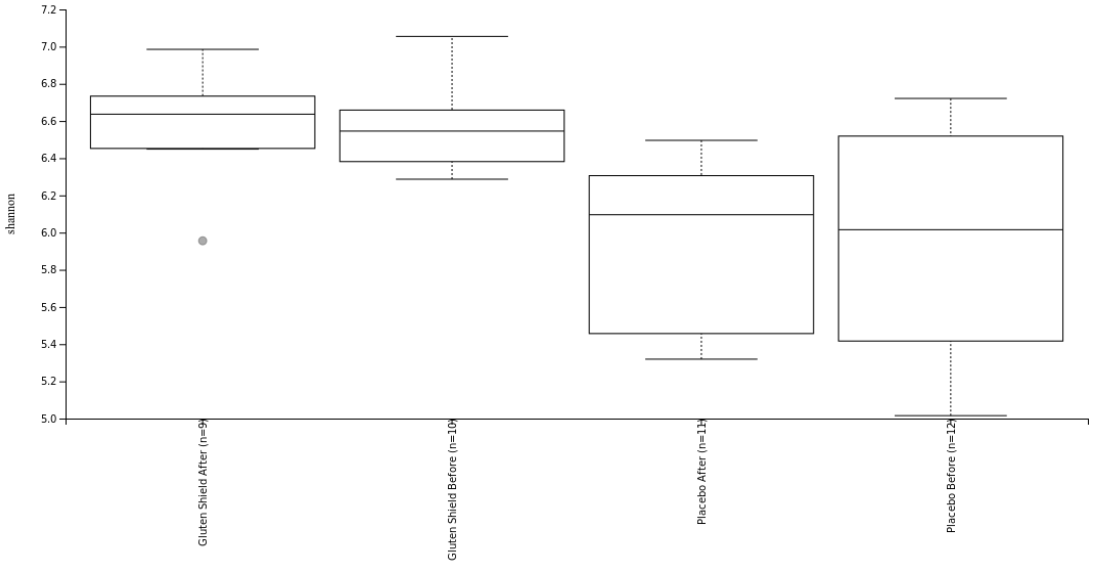

Figure 3: Shannon's diversity index (y-axis) for experimental and control groups before and after Glutenshield supplementation. Dots represent statistical outliers.

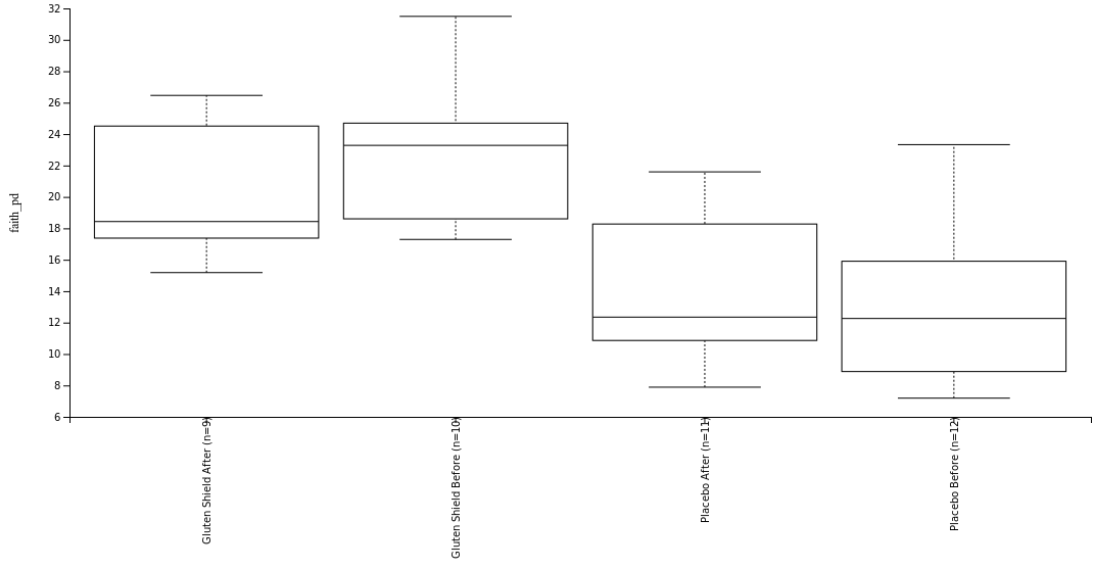

Figure 4: Faith's phylogenetic diversity (y-axis) for experimental and control groups before after Glutenshield supplementation.

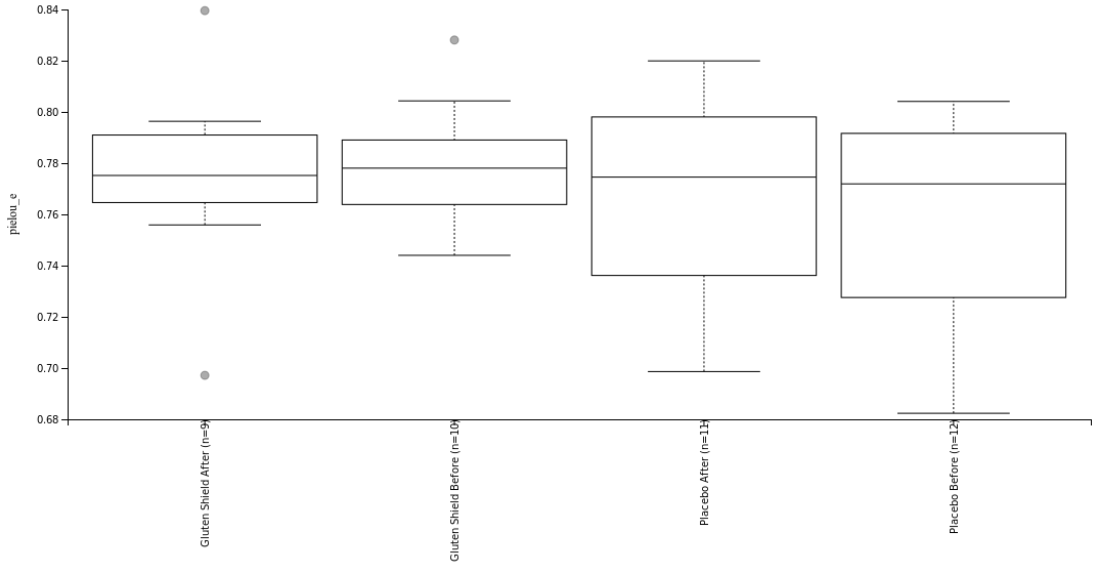

Figure 5: Pielou's Evenness (y-axis) for experimental and control groups before and after Glutenshield supplementation. Dots represent statistical outliers.

3.1.3 Immune Markers

Richness and evenness metrics were negatively correlated with serum IgG4 levels (Shannon r_s=-0.46, p=0.0022; OTUs r_s=-0.38 p=0.014; Faith r_s=-0.32, p=0.042; Pielou r_s=-0.41, p=0.0067) (Figure 6). Shannon's diversity (r_s=0.37, p=0.0477) and Pielou's evenness correlated with serum IgM (r_s=0.34, p=0.028) (Figure 7). IL-2 correlated with the number of observed OTUs per sample (r_s=0.314, p=0.0426). IgG1, IgG2, IgG3, IgA, IL-6, IL-8, and TNF-α did not correlate with any alpha diversity metrics (p>0.05) (Figures 6, 7).

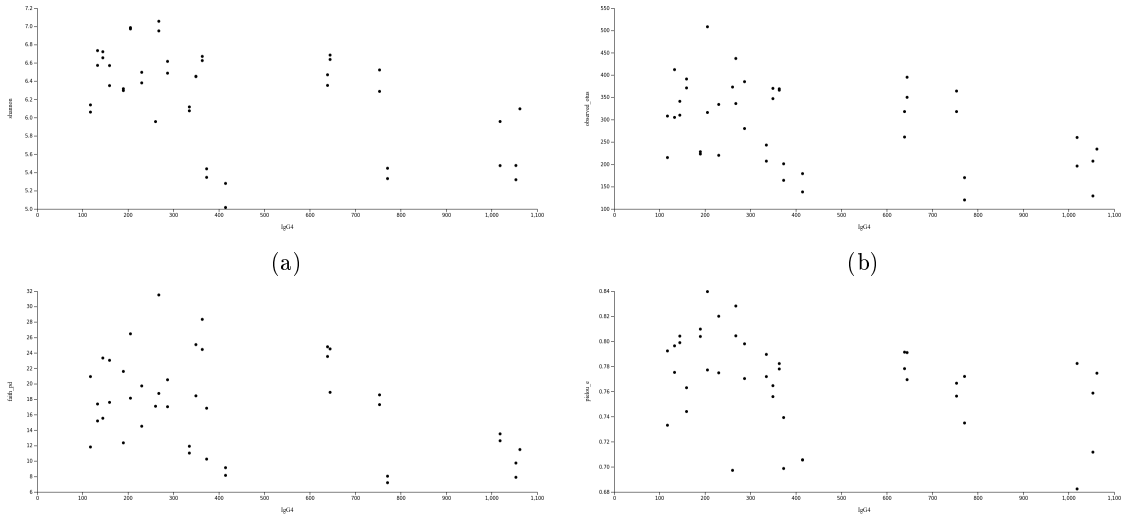

Figure 6: IgG4 (x-axes) plotted against y-axes of Shannon's diversity index (a), Observed OTUs (b), Faith's phylogenetic diversity (c), and Pielou's evenness (d). One dot represents one sequencing sample, with two sequencing samples per fecal sample.

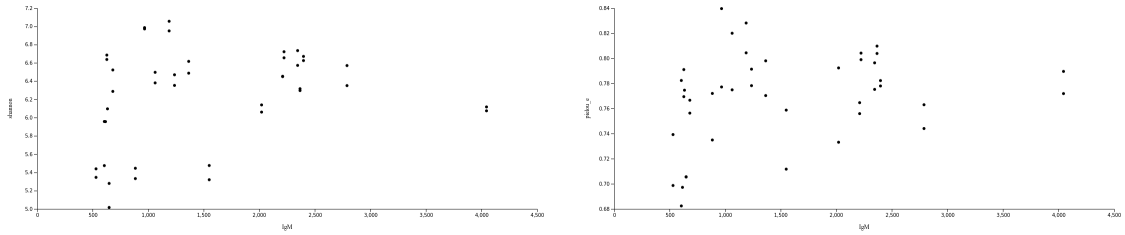

(a) (b)

Figure 7: IgM (x-axes) plotted against y-axes Shannon's diversity index (a) and Pielou's evenness (b). One dot represents one sequencing sample, with two sequencing samples per fecal sample.

3.1.4 Fecal Fiber and Protein

Faith's phylogenetic diversity positively correlated with total dietary fiber present in the fecal matter (r_s=0.304, p=0.05). Fecal crude protein correlated with Pielou's evenness (r_s=0.321, p=0.043) (Figure 8).

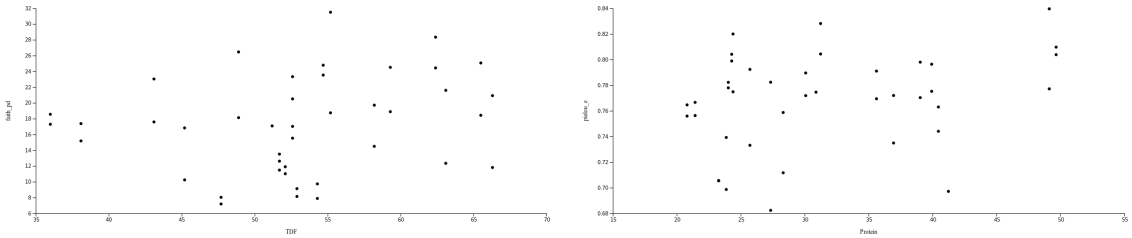

(a) (b)

Figure 8: Total dietary fiber present in feces (x-axis) plotted against y-axis Faith's phylogenetic diversity (a); crude protein present in feces (x-axis) plotted against y-axis Pielou's Evenness (b). One dot represents one sequencing sample, with two sequencing samples per fecal sample.

3.1.5 Fecal SCFA

The percent of the area under the curve (%AUC) of acetate correlated with Pielou's evenness (r_s=0.3530, p=0.0218). Propionate %AUC was strongly negatively correlated with richness and evenness (Shannon r_s=-0.6137, p=0.0000; OTUs r_s=-0.6298; Faith r_s=-0.5704, p=0.0001; Pielou r_s=-0.4038, p=0.008) (Figure 9). Isobutyrate %AUC correlated with qualitative measures of richness (OTUs r_s=0.3660, p=0.0171; Faith r_s=0.3449, p=0.0253) (Figure 10). Valerate %AUC correlated with observed OTUs (r_s=0.3475, p=0.021), and isovalerate %AUC correlated with Faith's phylogenetic diversity (r_s=0.3066, p=0.0483) (Figure 10). Caproate %AUC strongly correlated with richness but not evenness (Shannon's diversity r_s=0.5117, p=0.0005; OTUs r_s=0.6679, p<0.0001; Faith r_s=0.5142, p=0.0005; Pielou p>0.05) (Figure 11).

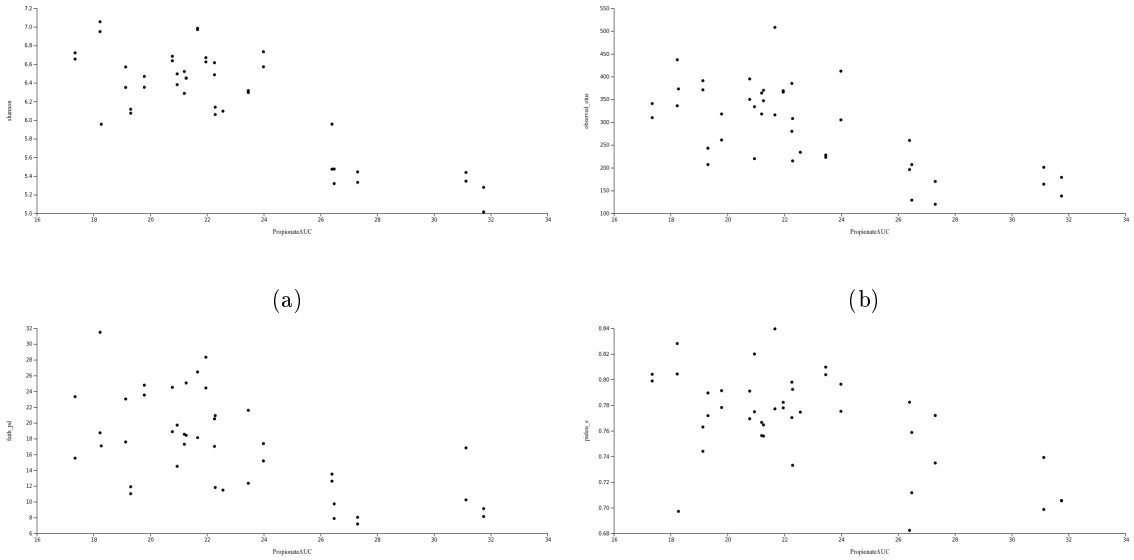

Figure 9: Propionate %AUC (x-axes) vs y-axes Shannon's diversity (a), Observed OTUs (b), Faith's phylogenetic diversity (c), and Pielou's evenness (d). One dot represents one sequencing sample, with two sequencing samples per fecal sample.

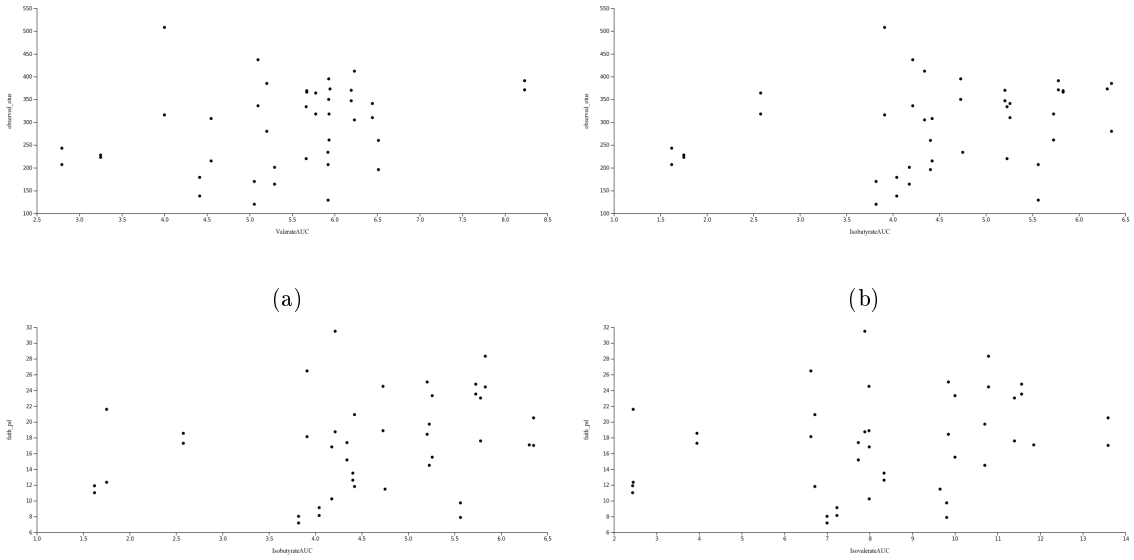

Figure 10: Valerate %AUC (x-axis) plotted against y-axis observed OTUs (a); isobutyrate %AUC (x-axis) plotted against y-axes observed OTUs (b) and Faith's phylogenetic diversity (c); isovalerate %AUC (x-axis) plotted against y-axis Faith's phylogenetic diversity (d). One dot represents one sequencing sample, with two sequencing samples per fecal sample.

Concentrations of fecal SCFA did not correlate as strongly as %AUC, as evidenced by fewer significant correlations and lower Spearman's rho values. Propionate and isobutyrate concentrations negatively correlated with evenness (r_s=-0.3058, p=0.0489; r_s=-0.3178, p=0.0403). Caproate concentrations, like AUC, did correlate with richness but not with evenness (Shannon r_s=0.4684, p=0.0018; OTUs r_s=0.6355, p<0.0001; Faith r_s=0.515, p=0.0005).

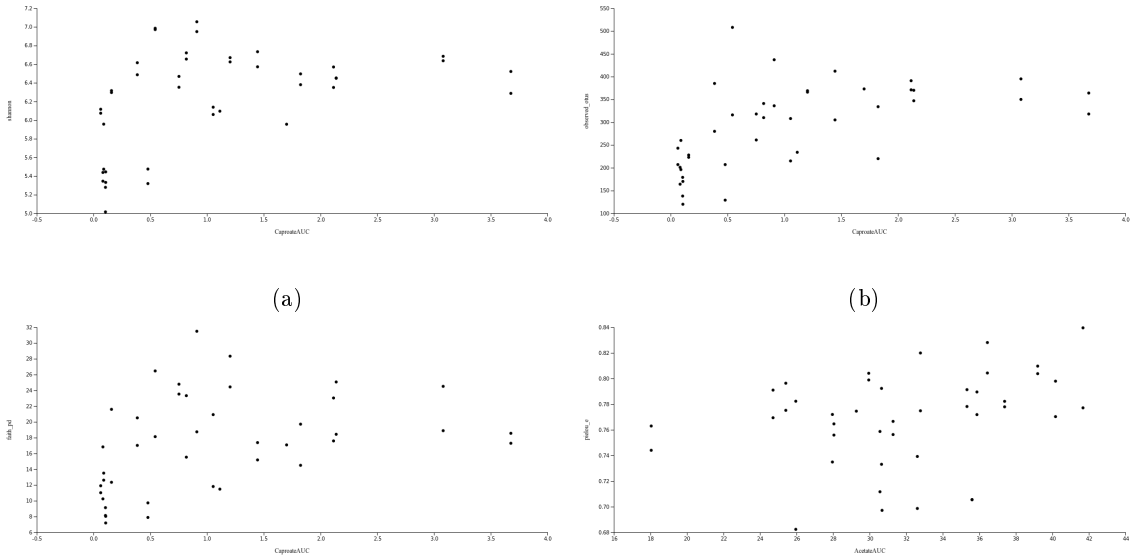

(a) (b)

(c) (d)

Figure 11: Caproate %AUC (x-axes) plotted against y-axes Shannon's diversity (a), Observed OTUs (b), Faith's phylogenetic diversity (c); Acetate %AUC (x-axis) plotted against y axis Pielou's Evenness (d). One dot represents one sequencing sample, with two sequencing samples per fecal sample.

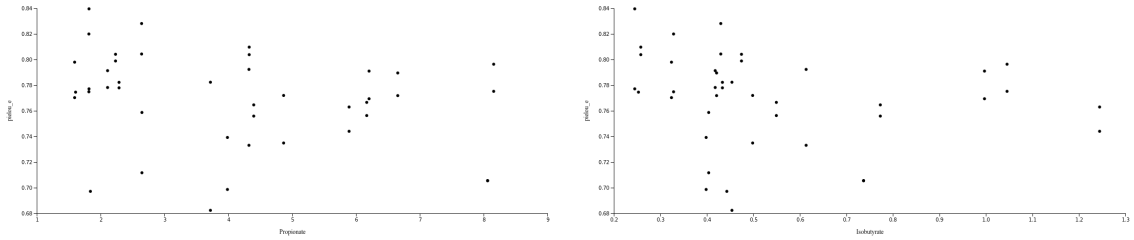

(a) (b)

Figure 12: Propionate concentration (a) plotted against y-axis Pielou's Evenness (a); isobutyrate concentration (x-axis) plotted against Pielou's Evenness (b). One dot represents one sequencing sample, with two sequencing samples per fecal sample.

3.1.6 Gastrointestinal Symptoms

Richness and evenness were negatively correlated with heartburn (Shannon r_s=-0.504, p=0.0007; OTUs r_s=-0.4494, p=0.0028; Faith r_s=-0.4016; Pielou r_s=-0.4216, p=0.0054). Urgent

need for defecation negatively correlated with Shannon's diversity index (r_s=-0.3672, p=0.0167) and Faith's phylogenetic diversity (r_s=-0.3317, p=0.0319). Feelings of incomplete evacuation positively correlated with all metrics of richness (Shannon r_s=0.5668, p=0.0001; OTUs r_s=0.5298, p=0.0003; Faith r_s=0.6026, p<0.0001). Eructation positively correlated with observed OTUs (r_s=0.3103, p=0.0455). No alpha diversity metrics correlated with acid regurgitation, bloating, nausea and vomiting, abdominal distension, increased gas, passage of stools, loose/hard stools, or the sum of all GI symptoms (p>0.05).

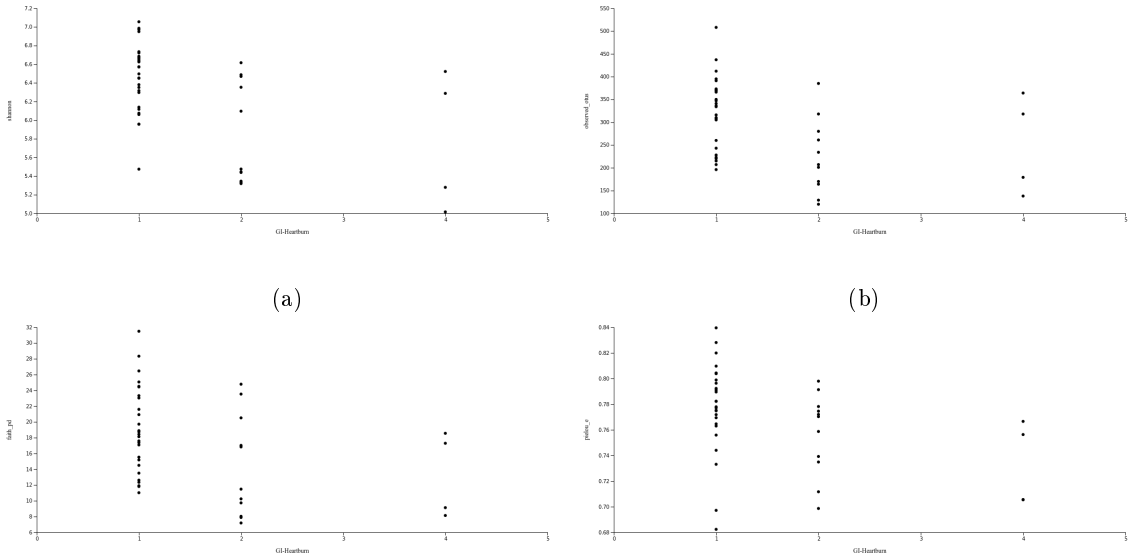

(a) (b)

(c) (d)

Figure 13: Heartburn (x-axes) plotted against y-axes Shannon's diversity (a), Observed OTUs (b), Faith's phylogenetic diversity (c); Acetate %AUC (x-axis) plotted against y-axis Pielou's Evenness (d). One dot represents one sequencing sample, with two sequencing samples per fecal sample.

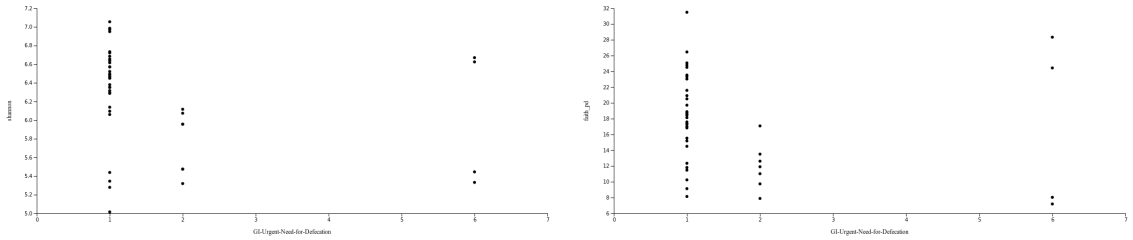

(a) (b)

Figure 14: Urgent need for defecation (x-axes) plotted against y-axes Shannon's diversity index (a) and Faith's phylogenetic diversity (b). One dot represents one sequencing sample, with two sequencing samples per fecal sample.

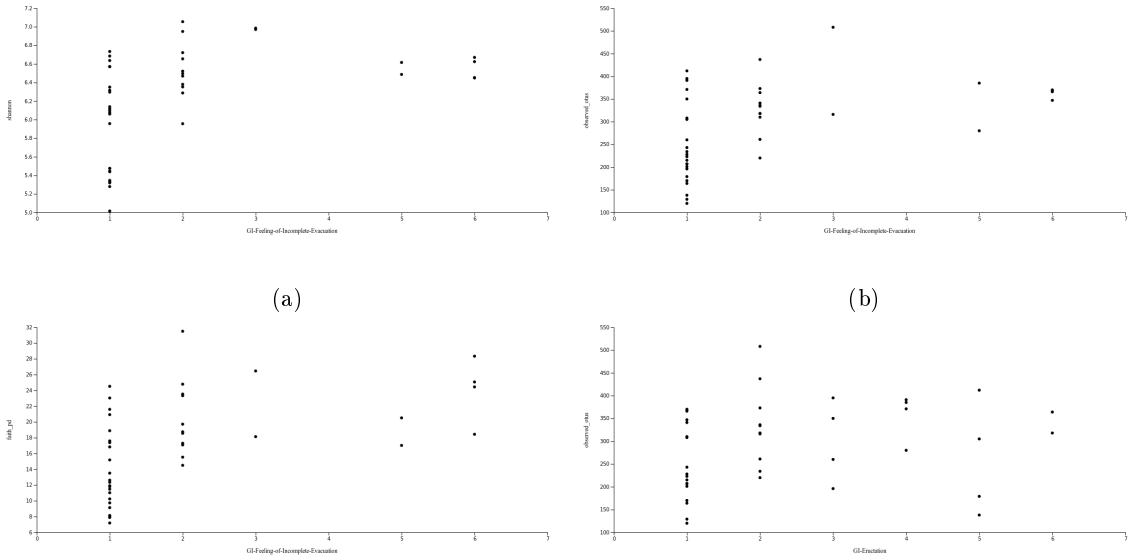

(a) (b)

(c) (d)

Figure 15: Feelings of incomplete evacuation (x-axes) plotted against y-axes Shannon's diversity (a), Observed OTUs (b), and Faith's phylogenetic diversity (c); eructation (x-axis) plotted against y-axis observed OTUs (d). One dot represents one sequencing sample, with two sequencing samples per fecal sample.

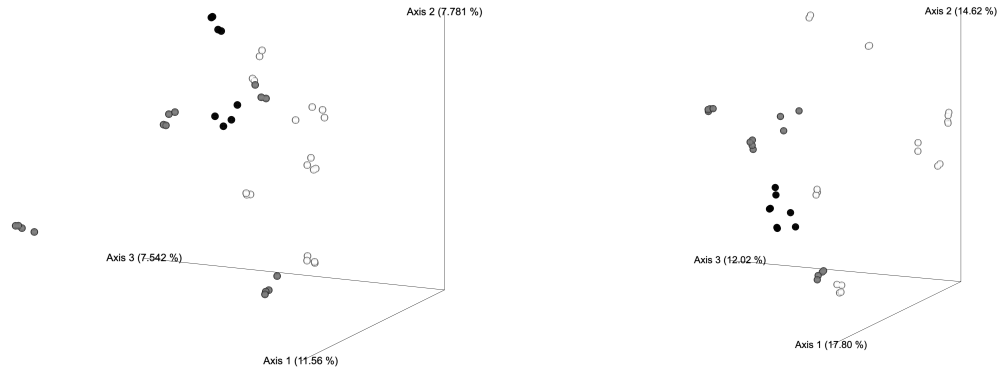

(a) (b)

Figure 16: Principle Coordinate Analysis (PCoA) plots based on Jaccard (a) and Bray-Curtis (b) generated distance matrices. Black points represent obese participants, grey represent overweight, and white represent normal BMI. Axes were chosen to represent as much variation as possible, and distances between points represent Euclidean distance. One point represents one sequencing sample, with two sequencing samples per fecal sample.

3.2 Beta Diversity

3.2.1 BMI

Significant differences were seen between BMI Classification groups for Jaccard distance, Bray-Curtis distance, and unweighted UniFrac but not for weighted Unifrac. Significant differences were seen from normal to overweight BMI groups (Jaccard p=0.001; Bray-Curtis p=0.001; unweighted UniFrac p=0.013), normal to obese (Jaccard p=0.001; Bray-Curtis p=0.001; unweighted UniFrac p=0.005), overweight to obese (Jaccard p=0.001; Bray-Curtis p=0.002; unweighted UniFrac p=0.016), and normal to overweight and obese combined (Jaccard p=0.001; Bray-Curtis p=0.001; unweighted UniFrac p=0.011).

3.2.2 Intervention

No metrics of beta diversity showed significant changes with Glutenshield or placebo supplementation ($p>0.05$).

3.2.3 Immune Markers

IgG1 correlated with Jaccard distance (r_s=0.17, p=0.012), and IgG3 correlated with unweighted UniFrac distance (r_s=0.156, p=0.047). IgG4 correlated with Jaccard distance (r_s=0.1878, p=0.013) and unweighted UniFrac distance (r_s=0.1368, p=0.032). IgA correlated with weighted UniFrac distance (r_s=0.2637, p=0.001), as did IL-8 (r_s=0.3064, p=0.001). IL-6 correlated with Bray-Curtis distance (r_s=0.1764, p=0.002).

3.2.4 Fecal Fiber and Protein

Insoluble dietary fiber content in the feces correlated with unweighted UniFrac distance (r_s=0.1482, p=0.04). Soluble and total dietary fiber content in feces correlated with weighted UniFrac distance (r_s=0.3526, p=0.001; r_s=0.1463, p=0.015). Protein did not correlate with any beta diversity metrics (p>0.05)

3.2.5 Fecal SCFA

Acetate %AUC correlated with qualitative beta diversity metrics Bray-Curtis (r_s=0.1389, p=0.025) and weighted UniFrac (r_s=0.2949, p=0.001). Propionate %AUC correlated with all metrics of beta diversity (Jaccard r_s=0.141, p=0.013; Bray-Curtis r_s=0.4910, p=0.001; unweighted UniFrac r_s=0.4016, p=0.001; weighted UniFrac r_s=0.2104, p=0.001). Butyrate %AUC correlated with multiple measures of beta diversity (Jaccard r_s=0.1656, p=0.003; Bray-Curtis r_s=0.1413, p=0.007; weighted UniFrac r_s=0.1521, p=0.007). Weighted UniFrac correlated with caproate %AUC (r_s=0.1241, p=0.044).

Propionate concentration correlated with Jaccard distance (r_s=0.1411, p=0.013), Bray-Curtis (r_s=0.1892, p=0.004), and weighted UniFrac (r_s=0.2649, p=0.002). Weighted UniFrac also correlated with butyrate (r_s=0.1707, p=0.003), isobutyrate (r_s=0.3475, p=0.001), valerate (r_s=0.4015, p=0.001), and isovalerate (r_s=0.3338, p=0.001) concentrations.

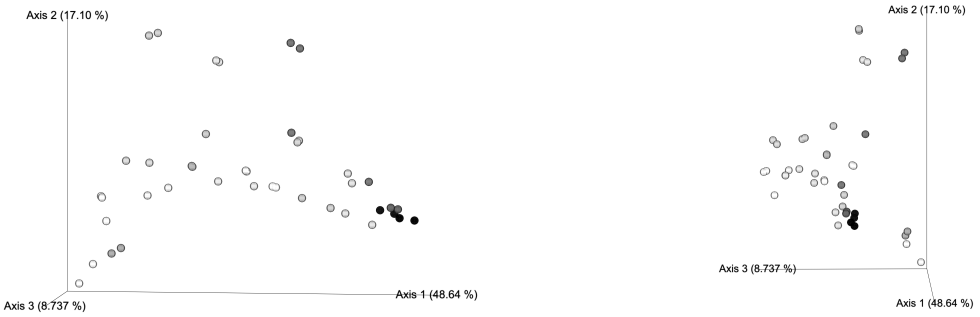

Figure 17: Rotated views of the same weighted UniFrac distance matrix PCoA plot. Darker points represent higher %AUC propionate. Axes were chosen to represent as much variation as possible, and distances between points represent Euclidean distance. One point represents one sequencing sample, with two sequencing samples per fecal sample.

3.2.6 Gastrointestinal Symptoms

Multiple gastrointestinal symptoms correlated with beta diversity metrics. Quantitative metrics Bray-Curtis and weighted UniFrac distance correlated with Heartburn (r_s=0.3192, p=0.002; r_s=0.1272, p=0.044). Phylogenetic metrics correlated with acid regurgitation (unweighted UniFrac r_s=0.2364, p=0.01; weighted UniFrac r_s=0.1799, p=0.02). Jaccard, Bray-Curtis, and unweighted UniFrac correlated with bloating (r_s=0.3098, p=0.001; r_s=0.2328, p=0.005; r_s=0.2763, p=0.001). Bray-Curtis correlated with nausea and vomiting (r_s=0.2494, p=0.012). All metrics correlated with abdominal distension(Jaccard r_s=0.2030, p=0.006; Bray-Curtis r_s=0.2045, p=0.007; unweighted UniFrac r_s=0.2056, p=0.003; weighted UniFrac r_s=0.1250, p=0.016) Quantitative metrics correlated with eructation (Bray-Curtis r_s=0.1615, p=0.026; weighted UniFrac r_s=0.2750, p=0.002). All metrics correlated with increased gas (Jaccard r_s=0.3130, p=0.001; Bray-Curtis r_s=0.2512, p=0.003; unweighted UniFrac r_s=0.2884, p=0.001; weighted UniFrac r_s=0.1563, p=0.015)

3.3 Taxonomy

The following taxonomy bar plots were generated using QIIME2:

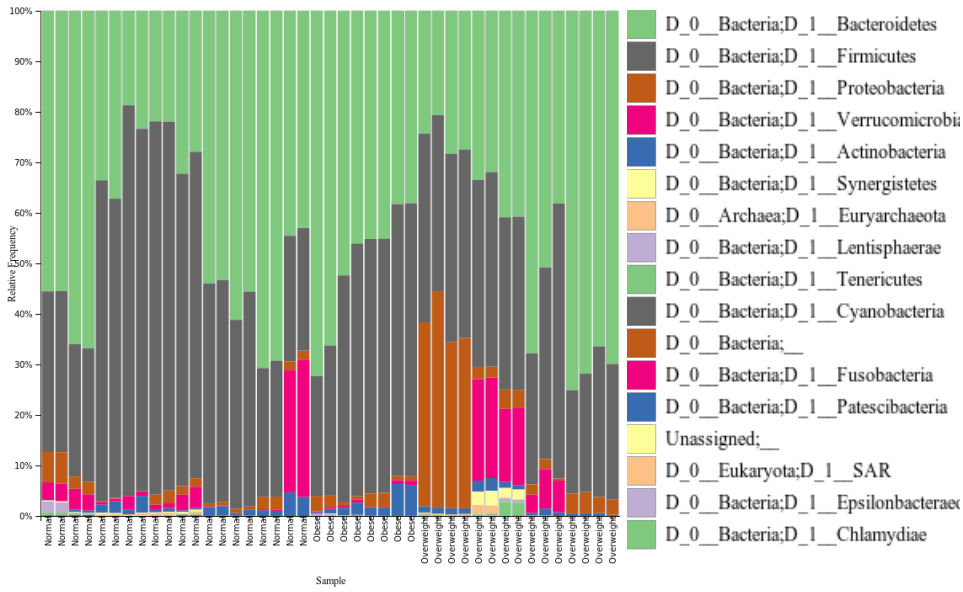

Figure 18: Taxonomic classification at the phylum level

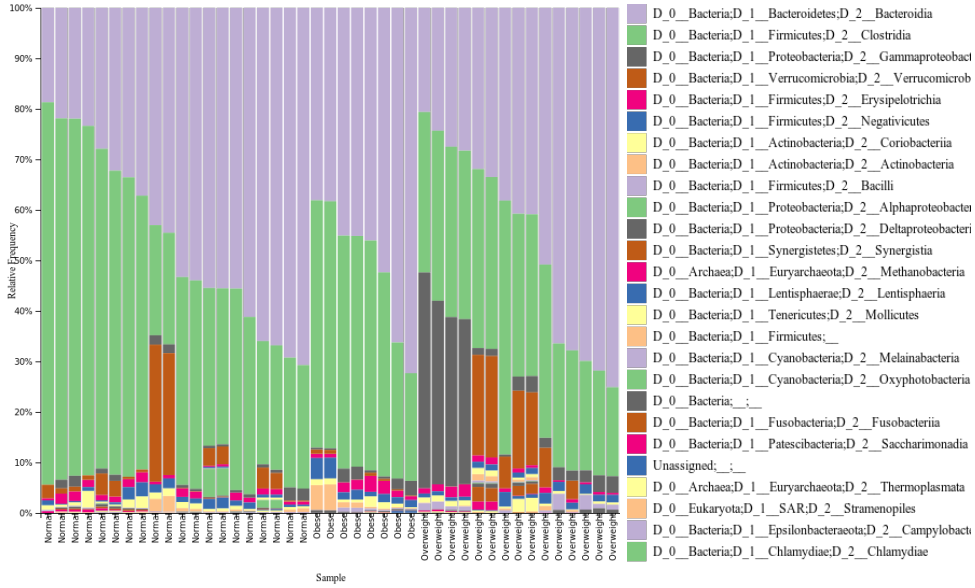

Figure 19: Taxonomic classification at the class level

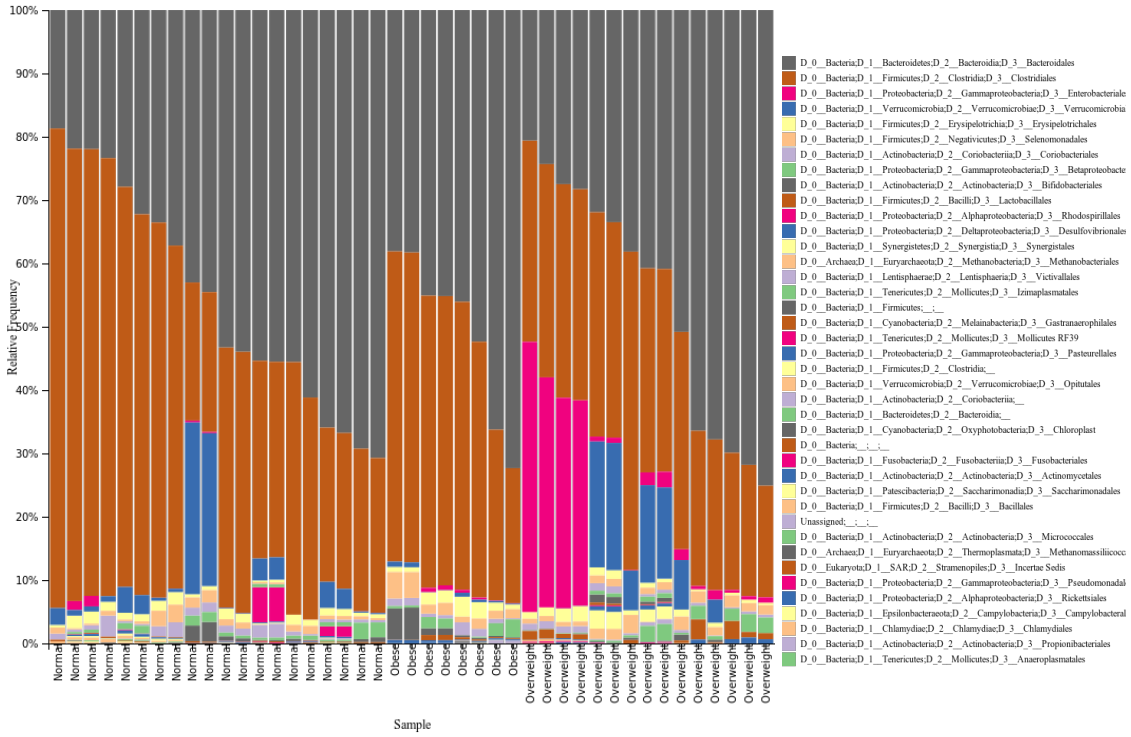

Figure 20: Taxonomic classification at the order level

3.4 Differential Abundances

Feaecalibacterium prausnitzii was found to be differentially abundant between BMI classification groups, with the highest abundance in the normal group and lowest abundance in the obese group (F=19.23, W=376). No other differentially abundant taxa showed trended from normal to obese BMI. At the species level, two members of the genus *Ruminoclostridium* were found to be differentially abundant, increasing more in the Glutenshield group than the placebo group (F=19.02, W=321; F=17.91, W=275). Members of the genus *Bifidobacterium* were also found to be differentially abundant, increasing more in the placebo supplementation group (F=12.21, W=176).

4 Discussion

4.1 BMI

The lack of difference in alpha diversity between BMI groups contrasts portions of the literature showing a negative correlation between alpha diversity and BMI [168, 169, 170]. However, studies demonstrating that link have had a much larger sample size than this one, or they have been performed with more controlling factors, such as using obese and lean twins [169]. This should serve as a reminder that though obesity is associated with chronic inflammation, metabolic disorders, and a microbiota trending toward dysbiosis, it is most directly a result of caloric imbalance [171]. However, the differences in beta diversity show evidence that different BMI groups have separate microbiome profiles, which does coincide with much of the literature [168, 169, 170]. The increased abundance of *Faecalibacterium prausnitzii* as BMI trended toward the normal group supports an association between *F prausnitzii* and a healthy weigh, but other studies have not shown consistent results. Results from other studies have demonstrated increased *F. prausnitzii* in obese children, no relationship between *F. prausnitzii* and obesity in adults, and decreased *F. prausnitzii* in obese individuals, so there is not a common consensus of the connections between *F. prausnitzii* and obesity [172, 173, 174] . The lack of *F. prausnitzii* in the microbiota of overweight and obese participants could suggest a potential mechanism for increased inflammation in obese individuals, as *F. prausnitzii* is a butyrate producer with anti-inflammatory properties [175, 176].

4.2 Intervention

Synbiotic supplementation did not yield significant changes to alpha or beta diversity, which could - at surface level - potentially cause one to believe it was an ineffective. However, other probiotic supplementation trials have shown supplementation to modify certain taxa without modifying the large-scale diversity of the microbiota [177]. The results of Webb et al 2019 demonstrated effectiveness of Glutenshield in this study for reducing IgG2 and bloating, suggesting that these results can be achieved without significantly modifying the microbiota

diversity, potentially by mechanisms such as antigen exposure without colonization. There is the possibility that due to manufacturing or structural issues with the probiotic, strains may not have been alive by the time the reached the colon, and these issues should be brought into question. It is known that even attenuated microbes of certain taxa can trigger physiological responses, especially members of the *Lactobacillus* and *Bifidobacterium* genera, which were included in Glutenshield [178, 179, 180]. Per the ANCOM results, Glutenshield supplementation did increase the abundance of *Ruminoclostridium* in the experimental group but not the control group. Higher abundances of *Ruminoclostridium* are found in patients without inflammatory bowel disease (IBD) compared to patients with IBD. *Ruminoclostridium* is in the family *Ruminocaccae*, which is a family containing obligate anaerobes including *Faecalibacterium*, which tends to be positively associated with health status [184].

One important factor that should be considered in future trials is the filler of the placebo supplement, as this likely had an effect on the microbiota of the control group, based on the differential abundance results of the ANCOM. It was found that *Bifidobacterium* were greatly increased upon supplementation of micro-crystalline cellulose, a dietary fiber, in the placebo group but not the Glutenshield group. Cellulose and cellodextrins (products of incomplete degradation of cellulose by other microbes) can be broken down by *Bifidobacterium*, and high cellulose diets have been shown to increase the abundance of *Bifidobacterium* in the gut microbiota [181, 182, 183]. It is possible that the effects of the placebo supplement on *Bifidobacterium* could have attentuated significant differences in changes in immune markers and symptoms between the control and experimental groups in Webb et al 2019 [136].

4.3 Immune Markers

The negative correlation between IgG4 and richness that was consistent across all metrics of alpha diversity suggests a strong relationship between the diversity of taxa present and IgG4 levels. IgG4 plays a role in the etiology of autoimmune diseases, and it has been found to be elevated in subsets of IBD patients [185]. Additionally, elevated IgG4 is associated with microbiota trending toward dysbiosis [185]. The results of this study also showed that IgG4 levels

correlated with qualitative metrics of beta diversity, suggesting that IgG4 elevation could be in response to the presence of different microbial profiles more dependent on presence and not as dependent on abundance of the differentially abundant taxa. Mechanistic links between microbiome diversity and IL-2 and IgM are yet to be elucidated, and associations with one metric of richness may not imply any causal relationship. The correlation of IgG1, IgG3, IgA, IL-6, and IL-8 suggest that participants with increased immune activation have different microbial communities compared to those with lower immune cytokine levels.

4.4 Fecal Fiber and Protein

Though the American Gut project found an association between the diversity of dietary fiber intake and alpha diversity, this study found a relationship between the total fiber present in the feces and Faith's phylogenetic diversity [17]. This relationship could exist due to increased total fiber intake potentially increasing the amount passed in the stool, and consumed fiber diversity may increase with increased total fiber consumed. The beta diversity correlation with soluble, insoluble, and total dietary fiber shows evidence for different communities in the microbiota of those with differing levels of fiber in the feces. This could be a result of multiple factors, such as recently altered fiber intake, high fiber intake, the lack of colonization by certain fiber-degrading species, or even faster transit time. It is known that dietary fiber plays an important role in shaping the gut microbiota, but this study did not control the many dimensions by which fiber intake can change [17].

Unfortunately, the relationship between fecal crude protein and evenness is not currently understood. Though certain taxa can utilize amino acids that escape digestion in the small intestine, microbial dynamics are complex, and more research is necessary to understand how the amount of fecal protein that passes through the stool is associated with evenness of the microbiome.

4.5 Fecal SCFA

The portion of the total SCFA that were propionate was strongly shown to decrease as richness decreased, suggesting that increased richness is associated with taxa that produce more complex SCFA. Similarly, as richness increased, the production of more complex SCFA, such as valerate, isovalerate, and caproate also increased, with caproate showing the strongest positive correlation with alpha diversity. Caproate concentration also correlated with alpha diversity, suggesting a potential application of caproate levels as a biomarker for alpha diversity in cases where it may be more applicable to measure SCFA ratios or concentrations than to sequence the microbiome. These results also supported another study showing that caproate and valerate levels are associated with increased richness [108]. Beta diversity correlations suggest that unique community structures are associated with varying amounts of each SCFA, which is supported by the fact that specific bacterial taxa harbor unique enzymes that degrade certain fibers to produce specific metabolites. Different bacterial communities will contain varying abundances of taxa that are capable of producing certain SCFA.

4.6 GI Symptoms

Many metrics of alpha and beta diversity were associated with gastrointestinal symptoms, reinforcing the role of microbial communities inflammatory bowel disease etiology. The inverse relationship between heartburn and richness supports a microbiota trending toward dysbiosis associating with the heartburn symptom presentation, which coincides with the high cooccurrence of IBD, functional dyspepsia, and gastroesophageal reflux disease [186].. It has been found that esophageal microbiota changes are associated with heartburn and esophageal reflux [187, 188]. However, since the gut microbiota and esophagus are separated by roughly 20 meters of small intestine with frequent peristaltic contractions and a stomach with pH around 3.5, it is unlikely that bacteria migrate from the gut microbiota to modulate the esophageal microbiome [189, 190]. There are multiple potential links between the gut microbiota and heartburn. One potential mechanistic link between the gut microbiota and heartburn could be the gut-vagus nerve axis,

which is a bidirectional (80% afferent) pathway that can be activated by specific microbial metabolites or by gut endocrine cells [191]. The vagal pathway is one of the most prevalent gut-brain axis pathways, and it also innervates the stomach and upper GI tract [192, 193]. Increased vagal activity is associated with esophageal acid reflux, which can trigger esophageal-cardiac reflex arcs that contribute to both cardiac and non-cardiac related angina-like chest pain [194, 193]. Another mechanism by which this could take place is by proton pump inhibitors (PPI), a common type of medication to reduce heartburn symptoms, altering the gut microbiota [195]. This study did not document the use of PPI by participants, which could have caused the observed microbiome changes associated in participants with heartburn. The correlation of beta diversity metrics with acid regurgitation and heartburn also suggest the association of differing microbial communities with upper GI symptoms, which could be the result of the aforementioned mechanisms.

Bloating and abdominal distension are symptoms of increased gas production in the small and large intestines, predominantly CO_2, H_2, and CH_4 [196]. The major source of intestinal gas is bacterial fermentation of undigested particles such as fibers and protein, and certain taxa are more likely to produce these gases, whereas other taxa are more likely to consume them [196]. Thus, it follows that this study found differences in the communities present with bloating, abdominal distension, and increased gas. Future testing will utilize numerical metadata differential abundance analyses to further elucidate what bacterial communities are more associated with gas and bloating.

The negative correlation between richness and urgent need to defecate and the positive correlation between richness and feelings of incomplete evacuation coincide with the literature characterizing the microbiota of constipated IBS patients (IBS-C). Though IBS patients generally experience a dysbiosis that is associated with low richness, IBS-C patients tend to have higher microbial richness and abundances [197, 198]. This is supported by studies demonstrating decreased richness in individuals with fast transit time and increased richness in individuals with slow transit time [199, 200].

4.7 Limitations

This study was limited by a small sample size. Though Webb 2019 had 20 participants, only the microbiomes of 11 participants (before and after) were able to be sequenced due to funding [136]. Also, the nature of most of the variables measured was observational and not causal, other than the effects of the placebo-controlled intervention. Limitations of the 16s microbiome analysis should also be considered. Despite the evolution of high-throughput sequencing and analysis techniques over the past 10 years, these methods do not fully reconstruct the microbiota of an individual - they only provide a representation [201]. Though denoising and chimera sorting were performed, these processes may not be perfect and may allow misreads and biases in the OTUs identified or excluded [202].

4.8 Future Directions

Future directions for this research include performing Songbird analysis to identify differentially abundant taxa for numerical metadata that correlated with beta-diversity in an effort to identify more specific differences in the communities present. Doing so may help to elucidate the microbiota changes associated with disease states, especially those of the gastrointestinal tract.

5 Conclusion

Overall, significant differences were found in community structure in participants with varying BMI classification and certain immune markers, fecal fiber, protein, and SCFA, and GI symptoms. Metrics of richness and evenness were found to significantly correlate with IgG4, IgM, IL-2, acetate, propionate, isobutyrate, valerate, isovalerate, caproate, heartburn, urgent need to defecate, and feelings of incomplete evacuation. Metrics of beta diversity distance between samples demonstrated significantly different community structure between normal and overweight, normal and obese, and overweight and obese BMI classification groups. Additionally, significant differences in community structure correlate with IgG1, IgG3, IgG4, IgA, IL-6, IL-8, fecal fiber, propionate, butyrate, heartburn, acid regurgitation, nausea and vomiting, bloating, abdominal

distension, increased gas, and eructation. Though metrics of alpha and beta diversity were not significantly altered by synbiotic intervention, an ANCOM identified differentially abundant bacterial taxa differentially abundant after supplementation. *Bifidobacterium* were increased in the placebo group, which could be a result of the placebo pill contents. The ANCOM also identified taxa associated with BMI. Findings demonstrate alpha and beta diversity associations with various SCFAs, GI symptoms, immune markers, and BMI. The results of the placebo-controlled intervention suggest careful consideration of placebo contents moving forward.

6 Acknowledgements

This undergraduate thesis would not have been possible without the support of many individuals. I would like to acknowledge Dr. Andy Clark as a mentor for providing direction and support for this project and for helping me secure funding to attend the QIIME2 workshop at Colorado State University, Dr. Michelle Chandley as a second reader for her critiques and for putting the idea in my head to analyze microbiota associations with SCFA, Kaitlyn Webb for the initial data provided from the Glutenshield study, and Sarah Parkinson for assistance with the microbiome sequencing. This project would not have been possible without travel-, research-, and scholarship-based financial support from the ETSU Honors College and the College of Clinical and Rehabilitative Health Sciences, nor would it have been possible without the constant positive regard of my advisors Dr. Karen Kornweibel and Professor Mary Andreae.

7 Appendix

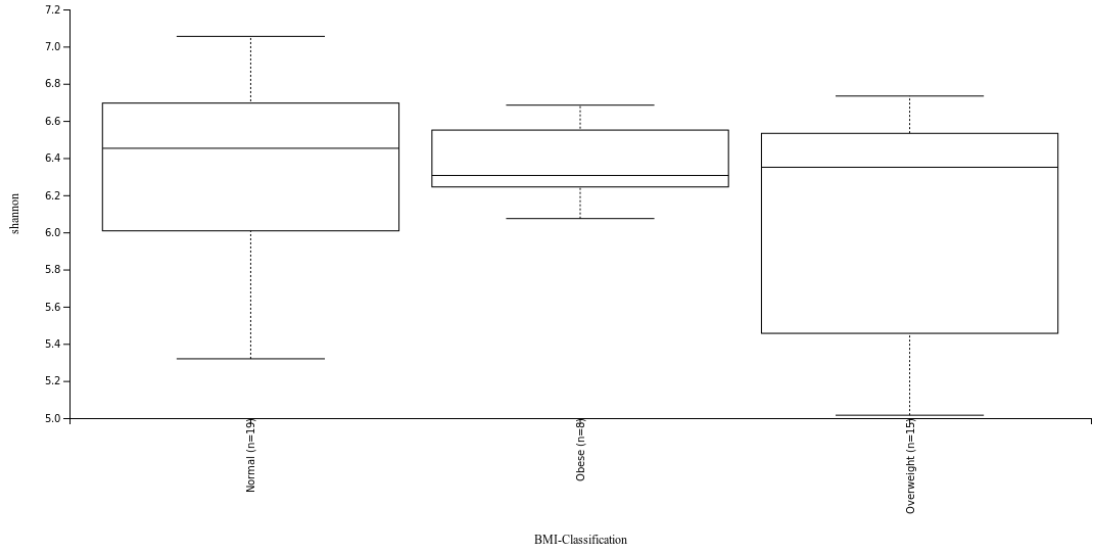

Figure 21: BMI classification (x-axis) plotted against Shannon's diversity index (y-axis).

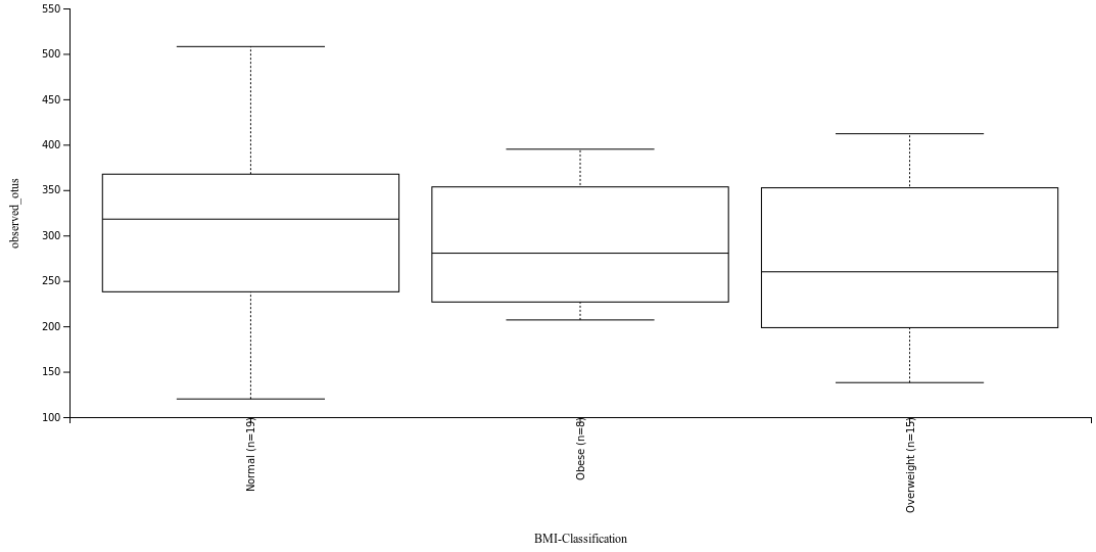

Figure 22: BMI classification (x-axis) plotted against observed OTUs (y-axis).

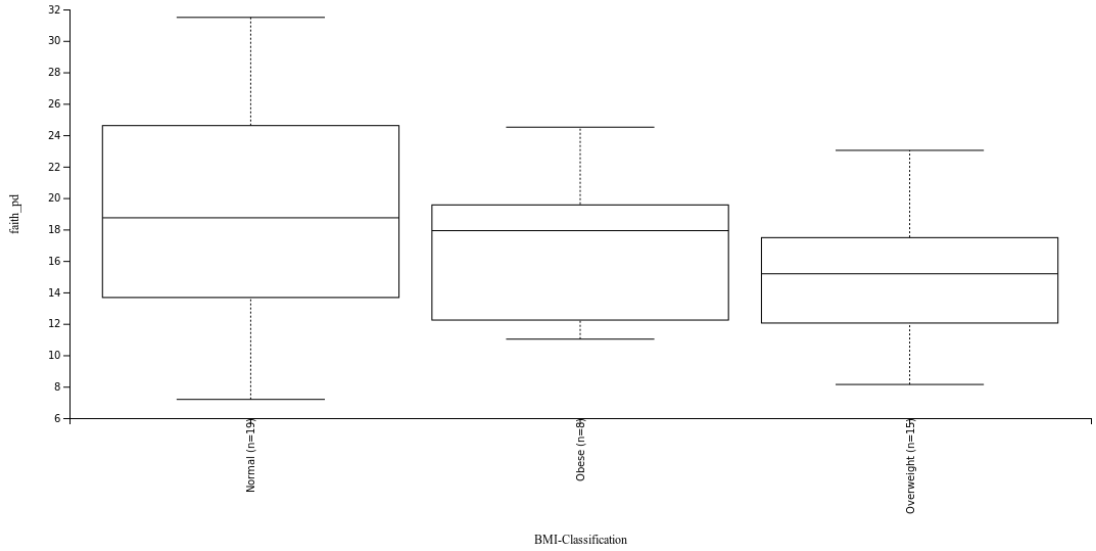

Figure 23: BMI classification (x-axis) plotted against Faith's phylogenetic diversity (y-axis).

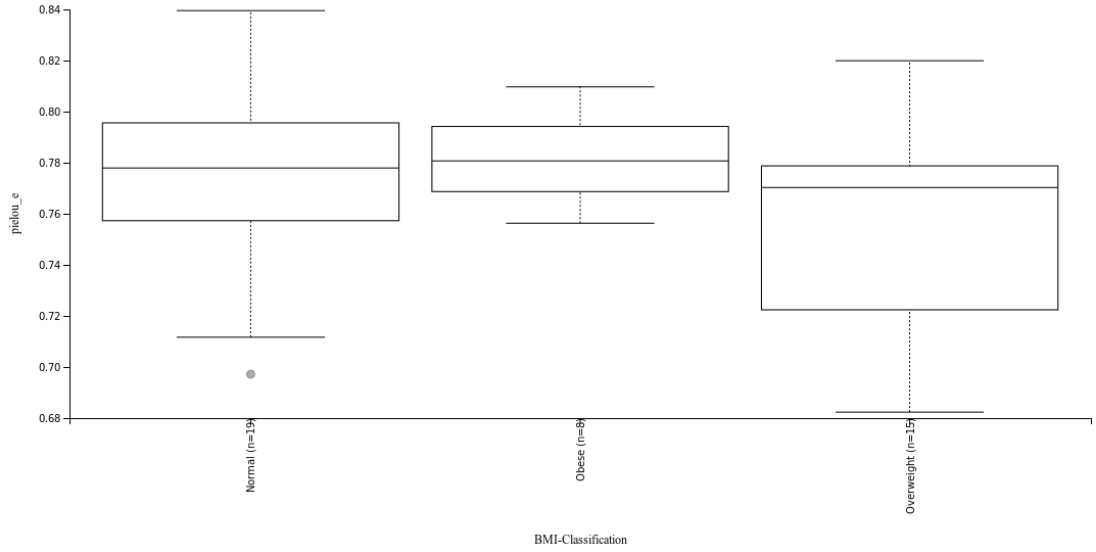

Figure 24: BMI classification (x-axis) plotted against Pielou's evenness (y-axis).

References

[1] Aleksej Zelezniak, Sergej Andrejev, Olga Ponomarova, Daniel R Mende, Peer Bork, and Kiran Raosaheb Patil. Metabolic dependencies drive species co-occurrence in diverse microbial communities. *Proceedings of the National Academy of Sciences*, 112(20):6449–6454, 2015.

[2] Sunil Thomas, Jacques Izard, Emily Walsh, Kristen Batich, Pakawat Chongsathidkiet, Gerard Clarke, David A Sela, Alexander J Muller, James M Mullin, Korin Albert, et al. The host microbiome regulates and maintains human health: a primer and perspective for non-microbiologists. *Cancer research*, 77(8):1783–1812, 2017.

[3] Luke K Ursell, Jessica L Metcalf, Laura Wegener Parfrey, and Rob Knight. Defining the human microbiome. *Nutrition reviews*, 70(suppl_1):S38–S44, 2012.

[4] Abigail C Allwood, Malcolm R Walter, Balz S Kamber, Craig P Marshall, and Ian W Burch. Stromatolite reef from the early archaean era of australia. *Nature*, 441(7094):714–718, 2006.

[5] Allan Konopka. What is microbial community ecology? *The ISME journal*, 3(11):1223–1230, 2009.

[6] Frederic Edward Clements. *Plant succession: an analysis of the development of vegetation*. Number 242. Carnegie Institution of Washington, 1916.

[7] Madhurankhi Goswami, Purnita Bhattacharyya, Indranil Mukherjee, and Prosun Tribedi. Functional diversity: An important measure of ecosystem functioning. *Advances in Microbiology*, 07, 10 2016.

[8] Norman W. H. Mason, David Mouillot, William G. Lee, and J. Bastow Wilson. Functional richness, functional evenness and functional divergence: the primary components of functional diversity. *Oikos*, 111(1):112–118, 2005.

[9] Hui Zhang, Robert John, Zechen Peng, Jianli Yuan, Chengjin Chu, Guozhen Du, and Shurong Zhou. The relationship between species richness and evenness in plant communities

along a successional gradient: a study from sub-alpine meadows of the eastern qinghai-tibetan plateau, china. *PloS one*, 7(11), 2012.

[10] Alessandra Riva, Orest Kuzyk, Erica Forsberg, Gary Siuzdak, Carina Pfann, Craig Herbold, Holger Daims, Alexander Loy, Benedikt Warth, and David Berry. A fiber-deprived diet disturbs the fine-scale spatial architecture of the murine colon microbiome. *Nature communications*, 10(1):1–11, 2019.

[11] Angela E Douglas. Symbiosis as a general principle in eukaryotic evolution. *Cold Spring Harbor Perspectives in Biology*, 6(2):a016113, 2014.

[12] Kelly P Williams, Bruno W Sobral, and Allan W Dickerman. A robust species tree for the alphaproteobacteria. *Journal of bacteriology*, 189(13):4578–4586, 2007.

[13] Thomas CG Bosch. Rethinking the role of immunity: lessons from hydra. *Trends in immunology*, 35(10):495–502, 2014.

[14] Ruth E Ley, Catherine A Lozupone, Micah Hamady, Rob Knight, and Jeffrey I Gordon. Worlds within worlds: evolution of the vertebrate gut microbiota. *Nature Reviews Microbiology*, 6(10):776–788, 2008.

[15] Curtis Huttenhower, Dirk Gevers, Rob Knight, Sahar Abubucker, Jonathan H Badger, Asif T Chinwalla, Heather H Creasy, Ashlee M Earl, Michael G FitzGerald, Robert S Fulton, et al. Structure, function and diversity of the healthy human microbiome. *nature*, 486(7402):207, 2012.

[16] Erwin G Zoetendal, Antoon DL Akkermans, and Willem M De Vos. Temperature gradient gel electrophoresis analysis of 16s rrna from human fecal samples reveals stable and host-specific communities of active bacteria. *Appl. Environ. Microbiol.*, 64(10):3854–3859, 1998.

[17] Daniel McDonald, Embriette Hyde, Justine W. Debelius, James T. Morton, Antonio Gonzalez, Gail Ackermann, Alexander A. Aksenov, Bahar Behsaz, Caitriona Brennan,

Yingfeng Chen, Lindsay DeRight Goldasich, Pieter C. Dorrestein, Robert R. Dunn, Ashkaan K. Fahimipour, James Gaffney, Jack A. Gilbert, Grant Gogul, Jessica L. Green, Philip Hugenholtz, Greg Humphrey, Curtis Huttenhower, Matthew A. Jackson, Stefan Janssen, Dilip V. Jeste, Lingjing Jiang, Scott T. Kelley, Dan Knights, Tomasz Kosciolek, Joshua Ladau, Jeff Leach, Clarisse Marotz, Dmitry Meleshko, Alexey V. Melnik, Jessica L. Metcalf, Hosein Mohimani, Emmanuel Montassier, Jose Navas-Molina, Tanya T. Nguyen, Shyamal Peddada, Pavel Pevzner, Katherine S. Pollard, Gholamali Rahnavard, Adam Robbins-Pianka, Naseer Sangwan, Joshua Shorenstein, Larry Smarr, Se Jin Song, Timothy Spector, Austin D. Swafford, Varykina G. Thackray, Luke R. Thompson, Anupriya Tripathi, Yoshiki Vázquez-Baeza, Alison Vrbanac, Paul Wischmeyer, Elaine Wolfe, Qiyun Zhu, , and Rob Knight. American gut: an open platform for citizen science microbiome research. *mSystems*, 3(3), 2018.

[18] Jonnelle M Edwards, Shaunak Roy, Jeremy C Tomcho, Zachary J Schreckenberger, Saroj Chakraborty, Nicole R Bearss, Piu Saha, Cameron G McCarthy, Matam Vijay-Kumar, Bina Joe, et al. Microbiota are critical for vascular physiology: Germ-free status weakens contractility and induces sex-specific vascular remodeling in mice. *Vascular pharmacology*, 125:106633, 2020.

[19] Parag Kundu, Hae Ung Lee, Isabel Garcia-Perez, Emmy Xue Yun Tay, Hyejin Kim, Llanto Elma Faylon, Katherine A. Martin, Rikky Purbojati, Daniela I. Drautz-Moses, Sujoy Ghosh, Jeremy K. Nicholson, Stephan Schuster, Elaine Holmes, and Sven Pettersson. Neurogenesis and prolongevity signaling in young germ-free mice transplanted with the gut microbiota of old mice. *Science Translational Medicine*, 11(518), 2019.

[20] Juliana Durack and Susan V Lynch. The gut microbiome: Relationships with disease and opportunities for therapy. *Journal of Experimental Medicine*, 216(1):20–40, 2019.

[21] Diego J. Castillo, Riaan F. Rifkin, Don A. Cowan, and Marnie Potgieter. The healthy human blood microbiome: Fact or fiction? *Frontiers in Cellular and Infection Microbiology*, 9:148, 2019.

[22] Junjie Qin, Ruiqiang Li, Jeroen Raes, Manimozhiyan Arumugam, Kristoffer Solvsten Burgdorf, Chaysavanh Manichanh, Trine Nielsen, Nicolas Pons, Florence Levenez, Takuji Yamada, et al. A human gut microbial gene catalogue established by metagenomic sequencing. *nature*, 464(7285):59–65, 2010.

[23] William B Whitman, David C Coleman, and William J Wiebe. Prokaryotes: the unseen majority. *Proceedings of the National Academy of Sciences*, 95(12):6578–6583, 1998.

[24] Ma Haynes, F Rohwer, and K Nelson. Metagenomics of the human body, 2011.

[25] PC Barko, MA McMichael, Kelly S Swanson, and David A Williams. The gastrointestinal microbiome: a review. *Journal of veterinary internal medicine*, 32(1):9–25, 2018.

[26] Jelena Štšepetova, Juliana Baranova, Jaak Simm, Ülle Parm, Tiiu Rööp, Sandra Sokmann, Paul Korrovits, Madis Jaagura, Karin Rosenstein, Andres Salumets, et al. The complex microbiome from native semen to embryo culture environment in human in vitro fertilization procedure. *Reproductive Biology and Endocrinology*, 18(1):1–13, 2020.

[27] Lisa F Stinson, Mary C Boyce, Matthew S Payne, and Jeffrey A Keelan. The not-so-sterile womb: evidence that the human fetus is exposed to bacteria prior to birth. *Frontiers in microbiology*, 10:1124, 2019.

[28] Inmaculada Moreno, Francisco M Codoñer, Felipe Vilella, Diana Valbuena, Juan F Martinez-Blanch, Jorge Jimenez-Almazán, Roberto Alonso, Pilar Alamá, Jose Remohí, Antonio Pellicer, et al. Evidence that the endometrial microbiota has an effect on implantation success or failure. *American journal of obstetrics and gynecology*, 215(6):684–703, 2016.

[29] I Crha, P Ventruba, J Žáková, M Ješeta, R Pilka, E Lousová, and Z Papíková. Uterine microbiome and endometrial receptivity. *Ceska gynekologie*, 84(1):49, 2019.

[30] Francisco Dominguez, Blanca Gadea, Amparo Mercader, Francisco J Esteban, Antonio Pellicer, and Carlos Simón. Embryologic outcome and secretome profile of implanted

blastocysts obtained after coculture in human endometrial epithelial cells versus the sequential system. *Fertility and sterility*, 93(3):774–782, 2010.

[31] John W Harris and J Howard Brown. The bacterial content of the uterus at cesarean section. *American Journal of Obstetrics & Gynecology*, 13(2):133–143, 1927.

[32] Matthew S Payne and Sara Bayatibojakhi. Exploring preterm birth as a polymicrobial disease: an overview of the uterine microbiome. *Frontiers in immunology*, 5:595, 2014.

[33] Kjersti Aagaard, Jun Ma, Kathleen M Antony, Radhika Ganu, Joseph Petrosino, and James Versalovic. The placenta harbors a unique microbiome. *Science translational medicine*, 6(237):237ra65–237ra65, 2014.

[34] Christian Milani, Sabrina Duranti, Francesca Bottacini, Eoghan Casey, Francesca Turroni, Jennifer Mahony, Clara Belzer, Susana Delgado Palacio, Silvia Arboleya Montes, Leonardo Mancabelli, et al. The first microbial colonizers of the human gut: composition, activities, and health implications of the infant gut microbiota. *Microbiol. Mol. Biol. Rev.*, 81(4):e00036–17, 2017.

[35] Esther Jiménez, María L Marín, Rocío Martín, Juan M Odriozola, Mónica Olivares, Jordi Xaus, Leonides Fernández, and Juan M Rodríguez. Is meconium from healthy newborns actually sterile? *Research in microbiology*, 159(3):187–193, 2008.

[36] Majda Dzidic, Alba Boix-Amorós, Marta Selma-Royo, Alex Mira, and Maria Carmen Collado. Gut microbiota and mucosal immunity in the neonate. *Medical Sciences*, 6(3):56, 2018.

[37] Charles M Cobb, Patricia J Kelly, Karen B Williams, Shilpa Babbar, Mubashir Angolkar, and Richard J Derman. The oral microbiome and adverse pregnancy outcomes. *International journal of women's health*, 9:551, 2017.

[38] Xue-Ru Wu, Tung-Tien Sun, and Juan J Medina. In vitro binding of type 1-fimbriated escherichia coli to uroplakins ia and ib: relation to urinary tract infections. *Proceedings of the National Academy of Sciences*, 93(18):9630–9635, 1996.

[39] Maria Carmen Collado, Samuli Rautava, Juhani Aakko, Erika Isolauri, and Seppo Salminen. Human gut colonisation may be initiated in utero by distinct microbial communities in the placenta and amniotic fluid. *Scientific reports*, 6:23129, 2016.

[40] Lorena Ruiz, Laura Moles, Miguel Gueimonde, and Juan M Rodriguez. Perinatal microbiomes' influence on preterm birth and preterms' health: influencing factors and modulation strategies. *Journal of pediatric gastroenterology and nutrition*, 63(6):e193–e203, 2016.

[41] Samuli Rautava, Raakel Luoto, Seppo Salminen, and Erika Isolauri. Microbial contact during pregnancy, intestinal colonization and human disease. *Nature reviews Gastroenterology & hepatology*, 9(10):565, 2012.

[42] Chen-Jian Liu, Xiao Liang, Zhao-Yi Niu, Qing Jin, Xue-Qin Zeng, Wen-Xue Wang, Meng-Yue Li, Xue-Rong Chen, Hai-Yun Meng, Ran Shen, et al. Is the delivery mode a critical factor for the microbial communities in the meconium? *EBioMedicine*, 49:354–363, 2019.

[43] Cian J Hill, Denise B Lynch, Kiera Murphy, Marynka Ulaszewska, Ian B Jeffery, Carol Anne O'Shea, Claire Watkins, Eugene Dempsey, Fulvio Mattivi, Kieran Tuohy, et al. Evolution of gut microbiota composition from birth to 24 weeks in the infantmet cohort. *Microbiome*, 5(1):4, 2017.

[44] Helena M Hesla, Fredrik Stenius, Lotta Jäderlund, Ronald Nelson, Lars Engstrand, Johan Alm, and Johan Dicksved. Impact of lifestyle on the gut microbiota of healthy infants and their mothers–the aladdin birth cohort. *FEMS microbiology ecology*, 90(3):791–801, 2014.

[45] Daniel Garrido, Santiago Ruiz-Moyano, Danielle G Lemay, David A Sela, J Bruce German, and David A Mills. Comparative transcriptomics reveals key differences in the response to

milk oligosaccharides of infant gut-associated bifidobacteria. *Scientific reports*, 5:13517, 2015.

[46] Christopher A Lowry, David G Smith, Philip H Siebler, Dominic Schmidt, Christopher E Stamper, James E Hassell, Paula S Yamashita, James H Fox, Stefan O Reber, Lisa A Brenner, et al. The microbiota, immunoregulation, and mental health: implications for public health. *Current environmental health reports*, 3(3):270–286, 2016.

[47] Lieve Desbonnet, Lillian Garrett, Gerard Clarke, Barry Kiely, John F Cryan, and Timothy G Dinan. Effects of the probiotic bifidobacterium infantis in the maternal separation model of depression. *Neuroscience*, 170(4):1179–1188, 2010.

[48] Tanya Yatsunenko, Federico E Rey, Mark J Manary, Indi Trehan, Maria Gloria Dominguez-Bello, Monica Contreras, Magda Magris, Glida Hidalgo, Robert N Baldassano, Andrey P Anokhin, et al. Human gut microbiome viewed across age and geography. *nature*, 486(7402):222–227, 2012.

[49] Valeria D'Argenio and Francesco Salvatore. The role of the gut microbiome in the healthy adult status. *Clinica chimica acta*, 451:97–102, 2015.

[50] Julia K Goodrich, Jillian L Waters, Angela C Poole, Jessica L Sutter, Omry Koren, Ran Blekhman, Michelle Beaumont, William Van Treuren, Rob Knight, Jordana T Bell, et al. Human genetics shape the gut microbiome. *Cell*, 159(4):789–799, 2014.

[51] Peter J Turnbaugh, Christopher Quince, Jeremiah J Faith, Alice C McHardy, Tanya Yatsunenko, Faheem Niazi, Jason Affourtit, Michael Egholm, Bernard Henrissat, Rob Knight, et al. Organismal, genetic, and transcriptional variation in the deeply sequenced gut microbiomes of identical twins. *Proceedings of the National Academy of Sciences*, 107(16):7503–7508, 2010.

[52] J Philip Karl, Adrienne M Hatch, Steven M Arcidiacono, Sarah C Pearce, Ida G Pantoja-Feliciano, Laurel A Doherty, and Jason W Soares. Effects of psychological,

environmental and physical stressors on the gut microbiota. *Frontiers in microbiology*, 9:2013, 2018.

[53] Harald Brüssow. Problems with the concept of gut microbiota dysbiosis. *Microbial biotechnology*, 13(2):423–434, 2020.

[54] Umberto Simeoni, Bernard Berger, Jana Junick, Michael Blaut, Sophie Pecquet, Enea Rezzonico, Dominik Grathwohl, Norbert Sprenger, Harald Brüssow, Study Team, et al. Gut microbiota analysis reveals a marked shift to bifidobacteria by a starter infant formula containing a synbiotic of bovine milk-derived oligosaccharides and b ifidobacterium animalis subsp. lactis cncm i-3446. *Environmental microbiology*, 18(7):2185–2195, 2016.

[55] April C Apostol, Kirk DC Jensen, and Anna E Beaudin. Training the fetal immune system through maternal inflammation—a layered hygiene hypothesis. *Frontiers in immunology*, 11:123, 2020.

[56] G Rook, Roberta Martinelli, and R Brunet. The 'old friends' hypothesis; how early contact with certain microorganisms may influence immunoregulatory circuits. *Perinatal Programming: Early Life Determinants of Adult Health & Disease. Taylor and Francis*, pages 183–194, 2005.

[57] Graham AW Rook, Christopher A Lowry, and Charles L Raison. Microbial 'old friends', immunoregulation and stress resilience. *Evolution, medicine, and public health*, 2013(1):46–64, 2013.

[58] GAW Rook and L ROSA Brunet. Chronic inflammatory disorders, the gut and "old friends" hypothesis. In *Inflammatory bowel disease: translation from basic research to clinical practice. Falk Symposium*, volume 140, pages 43–58, 2004.

[59] Tahli Singer-Englar, Gillian Barlow, and Ruchi Mathur. Obesity, diabetes, and the gut microbiome: an updated review. *Expert review of gastroenterology & hepatology*, 13(1):3–15, 2019.

[60] Kruttika Dabke, Gustaf Hendrick, and Suzanne Devkota. The gut microbiome and metabolic syndrome. *Journal of Clinical Investigation*, 129(10):4050–4057, 2019.

[61] Dominik Langgartner, Christopher A Lowry, and Stefan O Reber. Old friends, immunoregulation, and stress resilience. *Pflügers Archiv-European Journal of Physiology*, 471(2):237–269, 2019.

[62] Gijs den Besten, Karen van Eunen, Albert K Groen, Koen Venema, Dirk-Jan Reijngoud, and Barbara M Bakker. The role of short-chain fatty acids in the interplay between diet, gut microbiota, and host energy metabolism. *Journal of lipid research*, 54(9):2325–2340, 2013.

[63] Roy J Levin. Digestion and absorption of carbohydrates—from molecules and membranes to humans. *The American journal of clinical nutrition*, 59(3):690S–698S, 1994.

[64] Mahesh S Desai, Anna M Seekatz, Nicole M Koropatkin, Nobuhiko Kamada, Christina A Hickey, Mathis Wolter, Nicholas A Pudlo, Sho Kitamoto, Nicolas Terrapon, Arnaud Muller, et al. A dietary fiber-deprived gut microbiota degrades the colonic mucus barrier and enhances pathogen susceptibility. *Cell*, 167(5):1339–1353, 2016.

[65] Hannah D Holscher. Dietary fiber and prebiotics and the gastrointestinal microbiota. *Gut microbes*, 8(2):172–184, 2017.

[66] Julie Miller Jones. Codex-aligned dietary fiber definitions help to bridge the 'fiber gap'. *Nutrition journal*, 13(1):34, 2014.

[67] Johnson W McRorie and George C Fahey. A review of gastrointestinal physiology and the mechanisms underlying the health benefits of dietary fiber: matching an effective fiber with specific patient needs. *Clin Nurs Stud*, 1(4):82–92, 2013.

[68] Jonas Cremer, Igor Segota, Chih-yu Yang, Markus Arnoldini, John T Sauls, Zhongge Zhang, Edgar Gutierrez, Alex Groisman, and Terence Hwa. Effect of flow and peristaltic mixing on bacterial growth in a gut-like channel. *Proceedings of the National Academy of Sciences*, 113(41):11414–11419, 2016.

[69] Mattea Müller, Emanuel E Canfora, and Ellen E Blaak. Gastrointestinal transit time, glucose homeostasis and metabolic health: modulation by dietary fibers. *Nutrients*, 10(3):275, 2018.

[70] Doris Vandeputte, Gwen Falony, Sara Vieira-Silva, Raul Y Tito, Marie Joossens, and Jeroen Raes. Stool consistency is strongly associated with gut microbiota richness and composition, enterotypes and bacterial growth rates. *Gut*, 65(1):57–62, 2016.

[71] Markus Arnoldini, Jonas Cremer, and Terence Hwa. Bacterial growth, flow, and mixing shape human gut microbiota density and composition. *Gut microbes*, 9(6):559–566, 2018.

[72] Kristin A Verbeke, Alan R Boobis, Alessandro Chiodini, Christine A Edwards, Anne Franck, Michiel Kleerebezem, Arjen Nauta, Jeroen Raes, Eric AF Van Tol, and Kieran M Tuohy. Towards microbial fermentation metabolites as markers for health benefits of prebiotics. *Nutrition research reviews*, 28(1):42–66, 2015.

[73] Zhenyi Tian, Xiaojun Zhuang, Mei Luo, Wei Yin, and Lishou Xiong. The propionic acid and butyric acid in serum but not in feces are increased in patients with diarrhea-predominant irritable bowel syndrome. *BMC gastroenterology*, 20(1):1–8, 2020.

[74] John Hedley Cummings et al. *The large intestine in nutrition and disease*. Institut Danone Brussels, Belgium, 1997.

[75] David L Topping and Peter M Clifton. Short-chain fatty acids and human colonic function: roles of resistant starch and nonstarch polysaccharides. *Physiological reviews*, 81(3):1031–1064, 2001.

[76] Per G Farup, Knut Rudi, and Knut Hestad. Faecal short-chain fatty acids-a diagnostic biomarker for irritable bowel syndrome? *BMC gastroenterology*, 16(1):51, 2016.

[77] Emilia Hijova and Anna Chmelarova. Short chain fatty acids and colonic health. *Bratislavské lekárske listy*, 108(8):354, 2007.

[78] Jan Philipp Schuchardt and Andreas Hahn. Intestinal absorption and factors influencing bioavailability of magnesium-an update. *Current Nutrition & Food Science*, 13(4):260–278, 2017.

[79] Xiaojing Liu, Daniel E Cooper, Ahmad A Cluntun, Marc O Warmoes, Steven Zhao, Michael A Reid, Juan Liu, Peder J Lund, Mariana Lopes, Benjamin A Garcia, et al. Acetate production from glucose and coupling to mitochondrial metabolism in mammals. *Cell*, 175(2):502–513, 2018.

[80] Manuel A González Hernández, Emanuel E Canfora, Johan WE Jocken, and Ellen E Blaak. The short-chain fatty acid acetate in body weight control and insulin sensitivity. *Nutrients*, 11(8):1943, 2019.

[81] Rachel J Perry, Liang Peng, Natasha A Barry, Gary W Cline, Dongyan Zhang, Rebecca L Cardone, Kitt Falk Petersen, Richard G Kibbey, Andrew L Goodman, and Gerald I Shulman. Acetate mediates a microbiome–brain–β-cell axis to promote metabolic syndrome. *Nature*, 534(7606):213–217, 2016.

[82] Jéssica Aparecida da Silva Pereira, Felipe Corrêa da Silva, and Pedro Manoel Mendes de Moraes-Vieira. The impact of ghrelin in metabolic diseases: an immune perspective. *Journal of diabetes research*, 2017, 2017.

[83] Karolin Weitkunat, Sara Schumann, Daniela Nickel, Katharina Antonia Kappo, Klaus Jürgen Petzke, Anna Patricia Kipp, Michael Blaut, and Susanne Klaus. Importance of propionate for the repression of hepatic lipogenesis and improvement of insulin sensitivity in high-fat diet-induced obesity. *Molecular nutrition & food research*, 60(12):2611–2621, 2016.

[84] Hsu-Wen Chao, Shi-Wei Chao, Heng Lin, Hui-Chen Ku, and Ching-Feng Cheng. Homeostasis of glucose and lipid in non-alcoholic fatty liver disease. *International journal of molecular sciences*, 20(2):298, 2019.

[85] Yvonne Sun and Mary XD O'Riordan. Regulation of bacterial pathogenesis by intestinal short-chain fatty acids. 85:93–118, 2013.

[86] Federico E Rey, Jeremiah J Faith, James Bain, Michael J Muehlbauer, Robert D Stevens, Christopher B Newgard, and Jeffrey I Gordon. Dissecting the in vivo metabolic potential of two human gut acetogens. *Journal of biological chemistry*, 285(29):22082–22090, 2010.

[87] MEYER J Wolin and TERRY L Miller. Interactions of microbial populations in cellulose fermentation. In *Fed. Proc*, volume 42, pages 109–113, 1983.

[88] JE Bueld, G Bannenberg, and KJ Netter. Effects of propionic acid and pravastatin on hmg-coa reductase activity in relation to forestomach lesions in the rat. *Pharmacology & toxicology*, 78(4):229–234, 1996.

[89] Hans Ruppin, Simon Bar-Meir, Konrad H Soergel, Carol M Wood, and Milton G Schmitt. Absorption of short-chain fatty acids by the colon. *Gastroenterology*, 78(6):1500–1507, 1980.

[90] Filipe De Vadder, Petia Kovatcheva-Datchary, Daisy Goncalves, Jennifer Vinera, Carine Zitoun, Adeline Duchampt, Fredrik Bäckhed, and Gilles Mithieux. Microbiota-generated metabolites promote metabolic benefits via gut-brain neural circuits. *Cell*, 156(1-2):84–96, 2014.

[91] Nicholas Arpaia, Clarissa Campbell, Xiying Fan, Stanislav Dikiy, Joris van der Veeken, Paul Deroos, Hui Liu, Justin R Cross, Klaus Pfeffer, Paul J Coffer, et al. Metabolites produced by commensal bacteria promote peripheral regulatory t-cell generation. *Nature*, 504(7480):451–455, 2013.

[92] David Ríos-Covián, Patricia Ruas-Madiedo, Abelardo Margolles, Miguel Gueimonde, Clara G de los Reyes-Gavilán, and Nuria Salazar. Intestinal short chain fatty acids and their link with diet and human health. *Frontiers in microbiology*, 7:185, 2016.

[93] Amit Sharma and Dipayan Rudra. Emerging functions of regulatory t cells in tissue homeostasis. *Frontiers in immunology*, 9:883, 2018.

[94] Akiko Yamada, Rieko Arakaki, Masako Saito, Takaaki Tsunematsu, Yasusei Kudo, and Naozumi Ishimaru. Role of regulatory t cell in the pathogenesis of inflammatory bowel disease. *World journal of gastroenterology*, 22(7):2195, 2016.

[95] Jessica Harakal, Claudia Rival, Hui Qiao, and Kenneth S Tung. Regulatory t cells control th2-dominant murine autoimmune gastritis. *The Journal of Immunology*, 197(1):27–41, 2016.

[96] Andrew J Brown, Susan M Goldsworthy, Ashley A Barnes, Michelle M Eilert, Lili Tcheang, Dion Daniels, Alison I Muir, Mark J Wigglesworth, Ian Kinghorn, Neil J Fraser, et al. The orphan g protein-coupled receptors gpr41 and gpr43 are activated by propionate and other short chain carboxylic acids. *Journal of Biological Chemistry*, 278(13):11312–11319, 2003.

[97] Zhiwei Ang and Jeak Ling Ding. Gpr41 and gpr43 in obesity and inflammation–protective or causative? *Frontiers in immunology*, 7:28, 2016.

[98] Christina A Cherrington, M Hinton, GR Pearson, and I Chopra. Short-chain organic acids at ph 5.0 kill escherichia coli and salmonella spp. without causing membrane perturbation. *Journal of Applied Bacteriology*, 70(2):161–165, 1991.

[99] Dallas R Donohoe, Nikhil Garge, Xinxin Zhang, Wei Sun, Thomas M O'Connell, Maureen K Bunger, and Scott J Bultman. The microbiome and butyrate regulate energy metabolism and autophagy in the mammalian colon. *Cell metabolism*, 13(5):517–526, 2011.

[100] Svenja Plöger, Friederike Stumpff, Gregory B Penner, Jörg-Dieter Schulzke, Gotthold Gäbel, Holger Martens, Zanming Shen, Dorothee Günzel, and Joerg R Aschenbach. Microbial butyrate and its role for barrier function in the gastrointestinal tract. *Annals of the New York academy of sciences*, 1258(1):52–59, 2012.

[101] Bonggi Lee, Kyoung Mi Moon, and Choon Young Kim. Tight junction in the intestinal epithelium: Its association with diseases and regulation by phytochemicals. *Journal of immunology research*, 2018, 2018.

[102] Caleb J Kelly, Leon Zheng, Eric L Campbell, Bejan Saeedi, Carsten C Scholz, Amanda J Bayless, Kelly E Wilson, Louise E Glover, Douglas J Kominsky, Aaron Magnuson, et al. Crosstalk between microbiota-derived short-chain fatty acids and intestinal epithelial hif augments tissue barrier function. *Cell host & microbe*, 17(5):662–671, 2015.

[103] Henrike M Hamer, DMAE Jonkers, Koen Venema, SALW Vanhoutvin, FJ Troost, and R-J Brummer. The role of butyrate on colonic function. *Alimentary pharmacology & therapeutics*, 27(2):104–119, 2008.

[104] Charles L Raison, Christopher A Lowry, and Graham AW Rook. Inflammation, sanitation, and consternation: loss of contact with coevolved, tolerogenic microorganisms and the pathophysiology and treatment of major depression. *Archives of general psychiatry*, 67(12):1211–1224, 2010.

[105] Maik Luu, Sabine Pautz, Vanessa Kohl, Rajeev Singh, Rossana Romero, Sébastien Lucas, Jörg Hofmann, Hartmann Raifer, Niyati Vachharajani, Lucia Campos Carrascosa, et al. The short-chain fatty acid pentanoate suppresses autoimmunity by modulating the metabolic-epigenetic crosstalk in lymphocytes. *Nature communications*, 10(1):1–12, 2019.

[106] Meyer J Wolin. Volatile fatty acids and the inhibition of escherichia coli growth by rumen fluid. *Appl. Environ. Microbiol.*, 17(1):83–87, 1969.

[107] Julie AK McDonald, Benjamin H Mullish, Alexandros Pechlivanis, Zhigang Liu, Jerusa Brignardello, Dina Kao, Elaine Holmes, Jia V Li, Thomas B Clarke, Mark R Thursz, et al. Inhibiting growth of clostridioides difficile by restoring valerate, produced by the intestinal microbiota. *Gastroenterology*, 155(5):1495–1507, 2018.

[108] Julien Tap, Jean-Pierre Furet, Martine Bensaada, Catherine Philippe, Hubert Roth, Sylvie Rabot, Omar Lakhdari, Vincent Lombard, Bernard Henrissat, Gérard Corthier, et al. Gut microbiota richness promotes its stability upon increased dietary fibre intake in healthy adults. *Environmental microbiology*, 17(12):4954–4964, 2015.

[109] Ilias Lagkouvardos, Jörg Overmann, and Thomas Clavel. Cultured microbes represent a substantial fraction of the human and mouse gut microbiota. *Gut microbes*, 8(5):493–503, 2017.

[110] Jill E Clarridge. Impact of 16s rrna gene sequence analysis for identification of bacteria on clinical microbiology and infectious diseases. *Clinical microbiology reviews*, 17(4):840–862, 2004.

[111] Nancy J Ames, Alexandra Ranucci, Brad Moriyama, and Gwenyth R Wallen. The human microbiome and understanding the 16s rrna gene in translational nursing science. *Nursing research*, 66(2):184, 2017.

[112] Garold Fuks, Michael Elgart, Amnon Amir, Amit Zeisel, Peter J Turnbaugh, Yoav Soen, and Noam Shental. Combining 16s rrna gene variable regions enables high-resolution microbial community profiling. *Microbiome*, 6(1):17, 2018.

[113] Cristina Alcon-Giner, Shabhonam Caim, Suparna Mitra, Jennifer Ketskemety, Udo Wegmann, John Wain, Gusztav Belteki, Paul Clarke, and Lindsay J Hall. Optimisation of 16s rrna gut microbiota profiling of extremely low birth weight infants. *BMC genomics*, 18(1):841, 2017.

[114] Josef Wagner, Paul Coupland, Hilary P Browne, Trevor D Lawley, Suzanna C Francis, and Julian Parkhill. Evaluation of pacbio sequencing for full-length bacterial 16s rrna gene classification. *BMC microbiology*, 16(1):274, 2016.

[115] J Gregory Caporaso, Christian L Lauber, William A Walters, Donna Berg-Lyons, James Huntley, Noah Fierer, Sarah M Owens, Jason Betley, Louise Fraser, Markus Bauer, et al. Ultra-high-throughput microbial community analysis on the illumina hiseq and miseq platforms. *The ISME journal*, 6(8):1621–1624, 2012.

[116] James J Kozich, Sarah L Westcott, Nielson T Baxter, Sarah K Highlander, and Patrick D Schloss. Development of a dual-index sequencing strategy and curation pipeline for

analyzing amplicon sequence data on the miseq illumina sequencing platform. *Appl. Environ. Microbiol.*, 79(17):5112–5120, 2013.

[117] J Gregory Caporaso, Christian L Lauber, William A Walters, Donna Berg-Lyons, Catherine A Lozupone, Peter J Turnbaugh, Noah Fierer, and Rob Knight. Global patterns of 16s rrna diversity at a depth of millions of sequences per sample. *Proceedings of the national academy of sciences*, 108(Supplement 1):4516–4522, 2011.

[118] Raul Y Tito, Samuel Chaffron, Clara Caenepeel, Gipsi Lima-Mendez, Jun Wang, Sara Vieira-Silva, Gwen Falony, Falk Hildebrand, Youssef Darzi, Leen Rymenans, et al. Population-level analysis of blastocystis subtype prevalence and variation in the human gut microbiota. *Gut*, 68(7):1180–1189, 2019.

[119] Lucas Moitinho-Silva, Shaun Nielsen, Amnon Amir, Antonio Gonzalez, Gail L Ackermann, Carlo Cerrano, Carmen Astudillo-Garcia, Cole Easson, Detmer Sipkema, Fang Liu, et al. The sponge microbiome project. *Gigascience*, 6(10):gix077, 2017.

[120] Jack A. Gilbert, Janet K. Jansson, and Rob Knight. Earth microbiome project and global systems biology. *mSystems*, 3(3), 2018.

[121] Dillon MR Bokulich NA Abnet CC Al-Ghalith GA Alexander H Alm EJ Arumugam M Asnicar F Bai Y Bisanz JE Bittinger K Brejnrod A Brislawn CJ Brown CT Callahan BJ Caraballo-Rodríguez AM Chase J Cope EK Da Silva R Diener C Dorrestein PC Douglas GM Durall DM Duvallet C Edwardson CF Ernst M Estaki M Fouquier J Gauglitz JM Gibbons SM Gibson DL Gonzalez A Gorlick K Guo J Hillmann B Holmes S Holste H Huttenhower C Huttley GA Janssen S Jarmusch AK Jiang L Kaehler BD Kang KB Keefe CR Keim P Kelley ST Knights D Koester I Kosciolek T Kreps J Langille MGI Lee J Ley R Liu YX Loftfield E Lozupone C Maher M Marotz C Martin BD McDonald D McIver LJ Melnik AV Metcalf JL Morgan SC Morton JT Naimey AT Navas-Molina JA Nothias LF Orchanian SB Pearson T Peoples SL Petras D Preuss ML Pruesse E Rasmussen LB Rivers A Robeson MS Rosenthal P Segata N Shaffer M Shiffer A Sinha R Song SJ Spear JR Swafford

AD Thompson LR Torres PJ Trinh P Tripathi A Turnbaugh PJ Ul-Hasan S van der Hooft JJJ Vargas F Vázquez-Baeza Y Vogtmann E von Hippel M Walters W Wan Y Wang M Warren J Weber KC Williamson CHD Willis AD Xu ZZ Zaneveld JR Zhang Y Zhu Q Knight R Bolyen E, Rideout JR and Caporaso JG. Reproducible, interactive, scalable and extensible microbiome data science using qiime 2. *Nature Biotechnology*, 37:852–857, 2019.

[122] Benjamin J Callahan, Paul J McMurdie, Michael J Rosen, Andrew W Han, Amy Jo A Johnson, and Susan P Holmes. Dada2: high-resolution sample inference from illumina amplicon data. *Nature methods*, 13(7):581, 2016.

[123] Amnon Amir, Daniel McDonald, Jose A Navas-Molina, Evguenia Kopylova, James T Morton, Zhenjiang Zech Xu, Eric P Kightley, Luke R Thompson, Embriette R Hyde, Antonio Gonzalez, et al. Deblur rapidly resolves single-nucleotide community sequence patterns. *MSystems*, 2(2), 2017.

[124] Nicholas A Bokulich, Benjamin D Kaehler, Jai Ram Rideout, Matthew Dillon, Evan Bolyen, Rob Knight, Gavin A Huttley, and J Gregory Caporaso. Optimizing taxonomic classification of marker-gene amplicon sequences with qiime 2's q2-feature-classifier plugin. *Microbiome*, 6(1):90, 2018.

[125] Morgan N Price, Paramvir S Dehal, and Adam P Arkin. Fasttree 2–approximately maximum-likelihood trees for large alignments. *PloS one*, 5(3):e9490, 2010.

[126] Joseph P Zackular, Nielson T Baxter, Grace Y Chen, and Patrick D Schloss. Manipulation of the gut microbiota reveals role in colon tumorigenesis. *Msphere*, 1(1), 2016.

[127] Nicholas A Bokulich, Thomas S Collins, Chad Masarweh, Greg Allen, Hildegarde Heymann, Susan E Ebeler, and David A Mills. Associations among wine grape microbiome, metabolome, and fermentation behavior suggest microbial contribution to regional wine characteristics. *MBio*, 7(3):e00631–16, 2016.

[128] Claude E Shannon. A mathematical theory of communication. *Bell system technical journal*, 27(3):379–423, 1948.

[129] Daniel P Faith. Conservation evaluation and phylogenetic diversity. *Biological conservation*, 61(1):1–10, 1992.

[130] Evelyn C Pielou. The measurement of diversity in different types of biological collections. *Journal of theoretical biology*, 13:131–144, 1966.

[131] Paul Jaccard. The distribution of the flora in the alpine zone. 1. *New phytologist*, 11(2):37–50, 1912.

[132] Michael Greenacre and Raul Primicerio. *Multivariate analysis of ecological data*. Fundacion BBVA, 2014.

[133] JR Bray and JT Curtis. An ordination of upland forest communities of southern wisconsin. ecological monographs (27), 1957.

[134] Catherine Lozupone and Rob Knight. Unifrac: a new phylogenetic method for comparing microbial communities. *Appl. Environ. Microbiol.*, 71(12):8228–8235, 2005.

[135] Catherine A Lozupone, Micah Hamady, Scott T Kelley, and Rob Knight. Quantitative and qualitative β diversity measures lead to different insights into factors that structure microbial communities. *Appl. Environ. Microbiol.*, 73(5):1576–1585, 2007.

[136] Kaitlyn Webb. Effect of prebiotic, probiotic, and enzyme supplementation on gut fermentation, markers of inflammation and immune response in individuals with gi symptoms. 2019.

[137] Andreas Schwiertz, David Taras, Klaus Schäfer, Silvia Beijer, Nicolaas A Bos, Christiane Donus, and Philip D Hardt. Microbiota and scfa in lean and overweight healthy subjects. *Obesity*, 18(1):190–195, 2010.

[138] K Schäfer. Analysis of short chain fatty acids from different intestinal samples by capillary gas chromatography. *Chromatographia*, 40(9-10):550–556, 1995.

[139] Benjamin J Callahan, Paul J McMurdie, Michael J Rosen, Andrew W Han, Amy Jo A Johnson, and Susan P Holmes. Dada2: high-resolution sample inference from illumina amplicon data. *Nature methods*, 13(7):581, 2016.

[140] Kazutaka Katoh and Daron M Standley. Mafft multiple sequence alignment software version 7: improvements in performance and usability. *Molecular biology and evolution*, 30(4):772–780, 2013.

[141] DJ Lane. 16s/23s rrna sequencing. In E Stackebrandt and M Goodfellow, editors, *Nucleic Acid Techniques in Bacterial Systematics*, pages 115–175. John Wiley and Sons, New York, 1991.

[142] Morgan N Price, Paramvir S Dehal, and Adam P Arkin. Fasttree 2–approximately maximum-likelihood trees for large alignments. *PloS one*, 5(3):e9490, 2010.

[143] Daniel McDonald, Jose C Clemente, Justin Kuczynski, Jai Ram Rideout, Jesse Stombaugh, Doug Wendel, Andreas Wilke, Susan Huse, John Hufnagle, Folker Meyer, Rob Knight, and J Gregory Caporaso. The biological observation matrix (biom) format or: how i learned to stop worrying and love the ome-ome. *GigaScience*, 1(1):7, 2012.

[144] Daniel McDonald, Jose C Clemente, Justin Kuczynski, Jai Ram Rideout, Jesse Stombaugh, Doug Wendel, Andreas Wilke, Susan Huse, John Hufnagle, Folker Meyer, Rob Knight, and J Gregory Caporaso. The biological observation matrix (biom) format or: how i learned to stop worrying and love the ome-ome. *GigaScience*, 1(1):7, 2012.

[145] Daniel McDonald, Jose C Clemente, Justin Kuczynski, Jai Ram Rideout, Jesse Stombaugh, Doug Wendel, Andreas Wilke, Susan Huse, John Hufnagle, Folker Meyer, Rob Knight, and J Gregory Caporaso. The biological observation matrix (biom) format or: how i learned to stop worrying and love the ome-ome. *GigaScience*, 1(1):7, 2012.

[146] Daniel McDonald, Jose C Clemente, Justin Kuczynski, Jai Ram Rideout, Jesse Stombaugh, Doug Wendel, Andreas Wilke, Susan Huse, John Hufnagle, Folker Meyer, Rob Knight, and

J Gregory Caporaso. The biological observation matrix (biom) format or: how i learned to stop worrying and love the ome-ome. *GigaScience*, 1(1):7, 2012.

[147] Daniel P. Faith, Peter R. Minchin, and Lee Belbin. Compositional dissimilarity as a robust measure of ecological distance. *Vegetatio*, 69(1):57–68, 1987.

[148] Sophie Weiss, Zhenjiang Zech Xu, Shyamal Peddada, Amnon Amir, Kyle Bittinger, Antonio Gonzalez, Catherine Lozupone, Jesse R. Zaneveld, Yoshiki Vázquez-Baeza, Amanda Birmingham, Embriette R. Hyde, and Rob Knight. Normalization and microbial differential abundance strategies depend upon data characteristics. *Microbiome*, 5(1):27, Mar 2017.

[149] William H Kruskal and W Allen Wallis. Use of ranks in one-criterion variance analysis. *Journal of the American statistical Association*, 47(260):583–621, 1952.

[150] Wes McKinney. Data structures for statistical computing in python. In Stéfan van der Walt and Jarrod Millman, editors, *Proceedings of the 9th Python in Science Conference*, pages 51 – 56, 2010.

[151] Karl Pearson. Note on regression and inheritance in the case of two parents. *Proceedings of the Royal Society of London*, 58:240–242, 1895.

[152] Charles Spearman. The proof and measurement of association between two things. *The American journal of psychology*, 15(1):72–101, 1904.

[153] Nathan Mantel. The detection of disease clustering and a generalized regression approach. *Cancer research*, 27(2 Part 1):209–220, 1967.

[154] Karl Pearson. Note on regression and inheritance in the case of two parents. *Proceedings of the Royal Society of London*, 58:240–242, 1895.

[155] Charles Spearman. The proof and measurement of association between two things. *The American journal of psychology*, 15(1):72–101, 1904.

[156] Marti J Anderson. A new method for non-parametric multivariate analysis of variance. *Austral ecology*, 26(1):32–46, 2001.

[157] Yoshiki Vázquez-Baeza, Meg Pirrung, Antonio Gonzalez, and Rob Knight. Emperor: a tool for visualizing high-throughput microbial community data. *Gigascience*, 2(1):16, 2013.

[158] Yoshiki Vázquez-Baeza, Antonio Gonzalez, Larry Smarr, Daniel McDonald, James T Morton, Jose A Navas-Molina, and Rob Knight. Bringing the dynamic microbiome to life with animations. *Cell host and microbe*, 21(1):7–10, 2017.

[159] Pierre Legendre and Louis Legendre. *Numerical Ecology*, page 499. Elsevier, third edition, 2012.

[160] Nathan Halko, Per-Gunnar Martinsson, Yoel Shkolnisky, and Mark Tygert. An algorithm for the principal component analysis of large data sets. *arXiv e-prints*, 2010.

[161] Nicholas A. Bokulich, Benjamin D. Kaehler, Jai Ram Rideout, Matthew Dillon, Evan Bolyen, Rob Knight, Gavin A. Huttley, and J. Gregory Caporaso. Optimizing taxonomic classification of marker-gene amplicon sequences with qiime 2's q2-feature-classifier plugin. *Microbiome*, 6(1):90, 2018.

[162] Nicholas A. Bokulich, Benjamin D. Kaehler, Jai Ram Rideout, Matthew Dillon, Evan Bolyen, Rob Knight, Gavin A. Huttley, and J. Gregory Caporaso. Optimizing taxonomic classification of marker-gene amplicon sequences with qiime 2's q2-feature-classifier plugin. *Microbiome*, 6(1):90, 2018.

[163] Torbjørn Rognes, Tomáš Flouri, Ben Nichols, Christopher Quince, and Frédéric Mahé. Vsearch: a versatile open source tool for metagenomics. *PeerJ*, 4:e2584, 2016.

[164] Fabian Pedregosa, Gaël Varoquaux, Alexandre Gramfort, Vincent Michel, Bertrand Thirion, Olivier Grisel, Mathieu Blondel, Peter Prettenhofer, Ron Weiss, Vincent Dubourg, Jake Vanderplas, Alexandre Passos, David Cournapeau, Matthieu Brucher, Matthieu Perrot, and Édouard Duchesnay. Scikit-learn: Machine learning in python. *Journal of machine learning research*, 12(Oct):2825–2830, 2011.

[165] Fabian Pedregosa, Gaël Varoquaux, Alexandre Gramfort, Vincent Michel, Bertrand Thirion, Olivier Grisel, Mathieu Blondel, Peter Prettenhofer, Ron Weiss, Vincent Dubourg, Jake Vanderplas, Alexandre Passos, David Cournapeau, Matthieu Brucher, Matthieu Perrot, and Édouard Duchesnay. Scikit-learn: Machine learning in python. *Journal of machine learning research*, 12(Oct):2825–2830, 2011.

[166] Siddhartha Mandal, Will Van Treuren, Richard A White, Merete Eggesbø, Rob Knight, and Shyamal D Peddada. Analysis of composition of microbiomes: a novel method for studying microbial composition. *Microbial ecology in health and disease*, 26(1):27663, 2015.

[167] Siddhartha Mandal, Will Van Treuren, Richard A White, Merete Eggesbø, Rob Knight, and Shyamal D Peddada. Analysis of composition of microbiomes: a novel method for studying microbial composition. *Microbial ecology in health and disease*, 26(1):27663, 2015.

[168] Yeojun Yun, Han-Na Kim, Song E Kim, Seong Gu Heo, Yoosoo Chang, Seungho Ryu, Hocheol Shin, and Hyung-Lae Kim. Comparative analysis of gut microbiota associated with body mass index in a large korean cohort. *BMC microbiology*, 17(1):151, 2017.

[169] Peter J Turnbaugh, Micah Hamady, Tanya Yatsunenko, Brandi L Cantarel, Alexis Duncan, Ruth E Ley, Mitchell L Sogin, William J Jones, Bruce A Roe, Jason P Affourtit, et al. A core gut microbiome in obese and lean twins. *nature*, 457(7228):480–484, 2009.

[170] Brandilyn A Peters, Jean A Shapiro, Timothy R Church, George Miller, Chau Trinh-Shevrin, Elizabeth Yuen, Charles Friedlander, Richard B Hayes, and Jiyoung Ahn. A taxonomic signature of obesity in a large study of american adults. *Scientific reports*, 8(1):1–13, 2018.

[171] George A Bray, William E Heisel, Ashkan Afshin, Michael D Jensen, William H Dietz, Michael Long, Robert F Kushner, Stephen R Daniels, Thomas A Wadden, Adam G Tsai, et al. The science of obesity management: an endocrine society scientific statement. *Endocrine reviews*, 39(2):79–132, 2018.

[172] S Miquel, R Martin, O Rossi, LG Bermudez-Humaran, JM Chatel, H Sokol, M Thomas, JM Wells, and P Langella. Faecalibacterium prausnitzii and human intestinal health. *Current opinion in microbiology*, 16(3):255–261, 2013.

[173] Jie Feng, Huang Tang, Min Li, Xiaoyan Pang, Linghua Wang, Menghui Zhang, Yufeng Zhao, Xiaojun Zhang, and Jian Shen. The abundance of fecal faecalibacterium prausnitzii in relation to obesity and gender in chinese adults. *Archives of microbiology*, 196(1):73–77, 2014.

[174] Ramadass Balamurugan, Gemlyn George, Jayakanthan Kabeerdoss, Jancy Hepsiba, Aarthy MS Chandragunasekaran, and Balakrishnan S Ramakrishna. Quantitative differences in intestinal faecalibacterium prausnitzii in obese indian children. *British journal of nutrition*, 103(3):335–338, 2010.

[175] Paul Blatchford, Halina Stoklosinski, Sarah Eady, Alison Wallace, Christine Butts, Richard Gearry, Glenn Gibson, and Juliet Ansell. Consumption of kiwifruit capsules increases faecalibacterium prausnitzii abundance in functionally constipated individuals: a randomised controlled human trial. *Journal of nutritional science*, 6, 2017.

[176] Kumar Ganesan, Sookja Kim Chung, Jairam Vanamala, and Baojun Xu. Causal relationship between diet-induced gut microbiota changes and diabetes: A novel strategy to transplant faecalibacterium prausnitzii in preventing diabetes. *International journal of molecular sciences*, 19(12):3720, 2018.

[177] Tam TT Tran, Fabien J Cousin, Denise B Lynch, Ravi Menon, Jennifer Brulc, Jillian R-M Brown, Eileen O'Herlihy, Ludovica F Butto, Katie Power, Ian B Jeffery, et al. Prebiotic supplementation in frail older people affects specific gut microbiota taxa but not global diversity. *Microbiome*, 7(1):39, 2019.

[178] Clifford A Adams. The probiotic paradox: live and dead cells are biological response modifiers. *Nutrition research reviews*, 23(1):37–46, 2010.

[179] Núria Piqué, Mercedes Berlanga, and David Miñana-Galbis. Health benefits of heat-killed (tyndallized) probiotics: An overview. *International journal of molecular sciences*, 20(10):2534, 2019.

[180] Ralf Jäger, Alex E Mohr, Katie C Carpenter, Chad M Kerksick, Martin Purpura, Adel Moussa, Jeremy R Townsend, Manfred Lamprecht, Nicholas P West, Katherine Black, et al. International society of sports nutrition position stand: Probiotics. *Journal of the International Society of Sports Nutrition*, 16(1):62, 2019.

[181] Audrey Rivière, Marija Selak, David Lantin, Frédéric Leroy, and Luc De Vuyst. Bifidobacteria and butyrate-producing colon bacteria: importance and strategies for their stimulation in the human gut. *Frontiers in microbiology*, 7:979, 2016.

[182] Y Morishita and Y Konishi. Effects of high dietary cellulose on the large intestinal microflora and short-chain fatty acids in rats. *Letters in applied microbiology*, 19(6):433–435, 1994.

[183] Karina Pokusaeva, Gerald F Fitzgerald, and Douwe van Sinderen. Carbohydrate metabolism in bifidobacteria. *Genes & nutrition*, 6(3):285–306, 2011.

[184] Giorgio Gargari, Valentina Taverniti, Silvia Balzaretti, Chiara Ferrario, Claudio Gardana, Paolo Simonetti, and Simone Guglielmetti. Consumption of a bifidobacterium bifidum strain for 4 weeks modulates dominant intestinal bacterial taxa and fecal butyrate in healthy adults. *Appl. Environ. Microbiol.*, 82(19):5850–5859, 2016.

[185] Zhujun Wang, Min Zhu, Chengxin Luo, Jingxi Mu, Wenyan Zhang, Qin Ouyang, Hu Zhang, et al. High level of igg4 as a biomarker for a new subset of inflammatory bowel disease. *Scientific reports*, 8(1):1–11, 2018.

[186] Sanne Rasmussen, Trine Holm Jensen, Susanne Lund Henriksen, Peter Fentz Haastrup, Pia Veldt Larsen, Jens Søndergaard, and Dorte Ejg Jarbøl. Overlap of symptoms of gastroesophageal reflux disease, dyspepsia and irritable bowel syndrome in the general population. *Scandinavian journal of gastroenterology*, 50(2):162–169, 2015.

[187] Liying Yang, Noami Chaudhary, Jonathan Baghdadi, and Zhiheng Pei. Microbiome in reflux disorders and esophageal adenocarcinoma. *Cancer journal (Sudbury, Mass.)*, 20(3):207, 2014.

[188] Ikenna Okereke, Catherine Hamilton, Alison Wenholz, Vikram Jala, Thao Giang, Sandy Reynolds, Aaron Miller, and Richard Pyles. Associations of the microbiome and esophageal disease. *Journal of thoracic disease*, 11(Suppl 12):S1588, 2019.

[189] David I Soybel. Anatomy and physiology of the stomach. *Surgical Clinics*, 85(5):875–894, 2005.

[190] LT Weaver, S Austin, and TJ Cole. Small intestinal length: a factor essential for gut adaptation. *Gut*, 32(11):1321–1323, 1991.

[191] Bruno Bonaz, Thomas Bazin, and Sonia Pellissier. The vagus nerve at the interface of the microbiota-gut-brain axis. *Frontiers in neuroscience*, 12:49, 2018.

[192] Kirsteen N Browning, Simon Verheijden, and Guy E Boeckxstaens. The vagus nerve in appetite regulation, mood, and intestinal inflammation. *Gastroenterology*, 152(4):730–744, 2017.

[193] Dominik Linz, Mathias Hohl, Johanna Vollmar, Christian Ukena, Felix Mahfoud, and Michael Böhm. Atrial fibrillation and gastroesophageal reflux disease: the cardiogastric interaction. *Ep Europace*, 19(1):16–20, 2017.

[194] G Tougas, R Spaziani, S Hollerbach, V Djuric, C Pang, ARM Upton, EL Fallen, and MV Kamath. Cardiac autonomic function and oesophageal acid sensitivity in patients with non-cardiac chest pain. *Gut*, 49(5):706–712, 2001.

[195] Matthew A Jackson, Julia K Goodrich, Maria-Emanuela Maxan, Daniel E Freedberg, Julian A Abrams, Angela C Poole, Jessica L Sutter, Daphne Welter, Ruth E Ley, Jordana T Bell, et al. Proton pump inhibitors alter the composition of the gut microbiota. *Gut*, 65(5):749–756, 2016.

[196] Juan R Malagelada, Anna Accarino, and Fernando Azpiroz. Bloating and abdominal distension: old misconceptions and current knowledge. *American Journal of Gastroenterology*, 112(8):1221–1231, 2017.

[197] Toshifumi Ohkusa, Shigeo Koido, Yuriko Nishikawa, and Nobuhiro Sato. Gut microbiota and chronic constipation: A review and update. *Frontiers in medicine*, 6, 2019.

[198] Ian M Carroll, Tamar Ringel-Kulka, Jennica P Siddle, and Yehuda Ringel. Alterations in composition and diversity of the intestinal microbiota in patients with diarrhea-predominant irritable bowel syndrome. *Neurogastroenterology & Motility*, 24(6):521–e248, 2012.

[199] Xiaolong Ge, Wei Zhao, Chao Ding, Hongliang Tian, Lizhi Xu, Hongkan Wang, Ling Ni, Jun Jiang, Jianfeng Gong, Weiming Zhu, et al. Potential role of fecal microbiota from patients with slow transit constipation in the regulation of gastrointestinal motility. *Scientific reports*, 7(1):1–11, 2017.

[200] William Tottey, David Feria-Gervasio, Nadia Gaci, Brigitte Laillet, Estelle Pujos, Jean-François Martin, Jean-Louis Sebedio, Benoit Sion, Jean-François Jarrige, Monique Alric, et al. Colonic transit time is a driven force of the gut microbiota composition and metabolism: in vitro evidence. *Journal of neurogastroenterology and motility*, 23(1):124, 2017.

[201] Jethro S Johnson, Daniel J Spakowicz, Bo-Young Hong, Lauren M Petersen, Patrick Demkowicz, Lei Chen, Shana R Leopold, Blake M Hanson, Hanako O Agresta, Mark Gerstein, et al. Evaluation of 16s rrna gene sequencing for species and strain-level microbiome analysis. *Nature communications*, 10(1):1–11, 2019.

[202] Rachel Poretsky, Luis M Rodriguez-R, Chengwei Luo, Despina Tsementzi, and Konstantinos T Konstantinidis. Strengths and limitations of 16s rrna gene amplicon sequencing in revealing temporal microbial community dynamics. *PloS one*, 9(4), 2014.